

# Discovery of (*R*)-2-Amino-6-borono-2-(2-(piperidin-1-yl)ethyl)hexanoic Acid and Congeners As Highly Potent Inhibitors of Human Arginases I and II for Treatment of Myocardial Reperfusion Injury

Michael C. Van Zandt,<sup>\*,†</sup> Darren L. Whitehouse,<sup>†</sup> Adam Golebiowski,<sup>†</sup> Min Koo Ji,<sup>†</sup> Mingbao Zhang,<sup>†</sup> R. Paul Beckett,<sup>†</sup> G. Erik Jagdmann,<sup>†</sup> Todd R. Ryder,<sup>†</sup> Ryan Sheeler,<sup>†</sup> Monica Andreoli,<sup>†</sup> Bruce Conway,<sup>†</sup> Keyvan Mahboubi,<sup>†</sup> Gerard D'Angelo,<sup>†</sup> Andre Mitschler,<sup>‡</sup> Alexandra Cousido-Siah,<sup>‡</sup> Francesc X. Ruiz,<sup>‡</sup> Eduardo I. Howard,<sup>‡,§</sup> Alberto D. Podjarny,<sup>‡</sup> and Hagen Schroeter<sup>||</sup>

<sup>†</sup>The Institutes for Pharmaceutical Discovery, LLC, 23 Business Park Drive, Branford, Connecticut 06405, United States

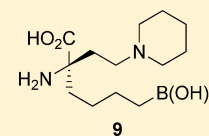
<sup>‡</sup>Department of Integrative Biology, IGBMC, CNRS, INSERM, Université de Strasbourg, 1 rue Laurent Fries, 67404 Illkirch, France

<sup>§</sup>IFLYSIB, Conicet, UNLP, Calle 59 N° 789, La Plata, Argentina

<sup>||</sup>Mars, Incorporated, 6885 Elm Street, McLean, Virginia 22101, United States

## **S** Supporting Information

**ABSTRACT:** Recent efforts to identify treatments for myocardial ischemia reperfusion injury have resulted in the discovery of a novel series of highly potent  $\alpha,\alpha$ -disubstituted amino acid-based arginase inhibitors. The lead candidate, (*R*)-2-amino-6-borono-2-(2-(piperidin-1-yl)ethyl)hexanoic acid, compound **9**, inhibits human arginases I and II with  $IC_{50}$ s of 223 and 509 nM, respectively, and is active in a recombinant cellular assay overexpressing human arginase I (CHO cells). It is 28% orally bioavailable and significantly reduces the infarct size in a rat model of myocardial ischemia/reperfusion injury. Herein, we report the design, synthesis, and structure–activity relationships (SAR) for this novel series of inhibitors along with pharmacokinetic and in vivo efficacy data for compound **9** and X-ray crystallography data for selected lead compounds cocrystallized with arginases I and II.



## ■ INTRODUCTION

Heart disease that leads to impaired blood flow and eventually a myocardial infarction or heart attack is the leading cause of death in the United States. Loss of blood flow to the heart, typically from a coronary arterial occlusion, leads to ischemia or lack of oxygen and nutrients and eventually death of heart tissue. Once circulation is restored, oxidative stress from formation of oxygen free radicals,<sup>1,2</sup> tissue damage from activated neutrophils,<sup>3</sup> apoptosis,<sup>4,5</sup> and calcium ion overload-induced myocyte hypercontracture<sup>6,7</sup> all contribute to reperfusion injury. The severity of tissue damage that results from the myocardial ischemia/reperfusion injury (MI/RI) is dependent on the duration of ischemia and the extent of microvascular dysfunction, inflammation, and oxidative stress sustained during injury. Significant damage to the myocardium can lead to reduced conduction velocities, arrhythmias and ventricular aneurysms, each with potentially catastrophic consequences. Reperfusion injury is a significant problem that affects millions of people each year. New treatments that improve patient outcomes are sorely needed.

The disease pathology of MI/RI is not completely understood but appears to be, at least, partially dependent on the metalloprotease arginase. Arginase expression levels and activity are increased in animal models of MI/RI.<sup>8</sup> Arginase catalyzes the manganese-mediated hydrolysis of L-arginine to

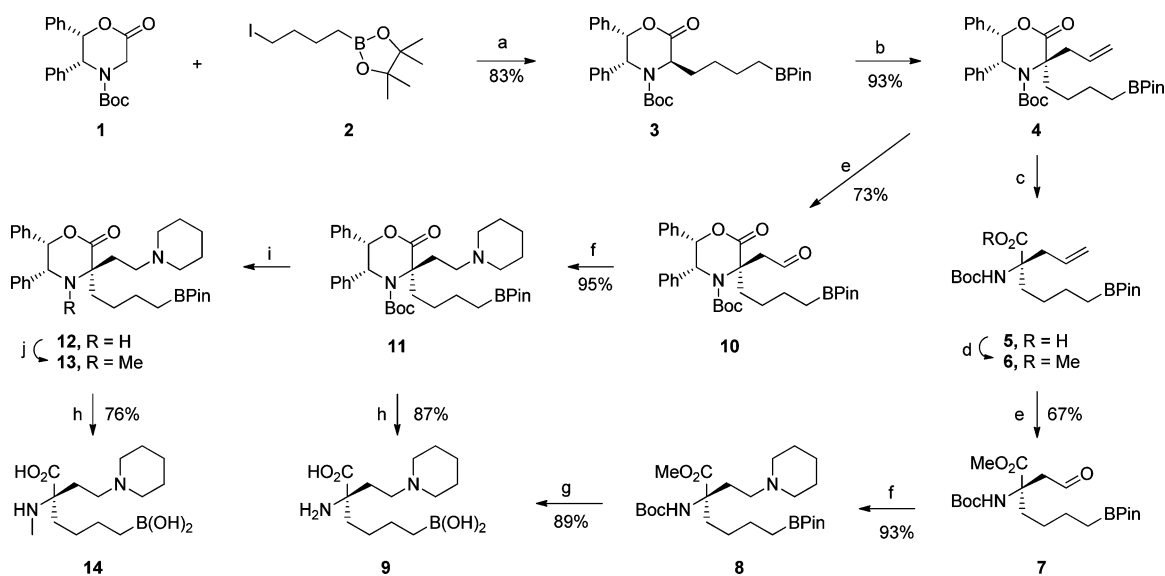
urea and L-ornithine. Because arginase and nitric oxide synthases (NOS) utilize arginine as a common substrate, upregulation of arginase may result in reduced levels of arginine and, consequently, decreased production of nitric oxide (NO), a physiologically important regulator of cardiac function.<sup>9</sup>

In addition to its potential role in regulating NO levels, arginase also affects production of critical polyamines such as putrescine, spermidine, and spermine. As arginase consumes arginine, it produces ornithine, which is subsequently converted to putrescine, spermidine, and spermine via the enzymes ornithine decarboxylase, spermidine synthase, and spermine synthase, respectively. These polyamines are important regulators of ion channels, protein synthesis, and cell viability. Thus, the arginase enzymes may control physiological signaling events by controlling the intracellular levels of NO and polyamine signal transducers.<sup>10</sup>

To date, much of the work in this area has been pioneered by the Christianson lab.<sup>11</sup> Their discovery of 2-(*S*)-amino-6-borono-hexanoic acid (ABH), one of the first significant arginase inhibitors, has made possible our current understanding of the role of arginase in various pathological states and its validation as an important therapeutic target.<sup>12,13</sup> On the

Received: January 3, 2013

Published: March 8, 2013

Scheme 1. Synthesis of  $\alpha,\alpha$ -Disubstituted Amino Acid Analogues<sup>a</sup>

<sup>a</sup>Reagents and conditions: (a) NaHMDS, HMPA, THF,  $-78\text{ }^{\circ}\text{C}$ ; (b) allyl iodide, KHMDS, DME,  $-78\text{ }^{\circ}\text{C}$ ; (c) Li,  $\text{NH}_3$ ; (d)  $\text{TMSCH}_2\text{N}_2$ , MeOH; (e) *i.* ozone,  $\text{CH}_2\text{Cl}_2$ ,  $-78\text{ }^{\circ}\text{C}$ , *ii.*  $\text{PPh}_3$ , 4 h; (f) piperidine,  $\text{NaBH}(\text{OAc})_3$ , AcOH,  $\text{CH}_2\text{Cl}_2$ ; (g) 6 N HCl,  $95\text{ }^{\circ}\text{C}$ , 12 h; (h) 6 N HCl, AcOH,  $\text{H}_2\text{O}$  then 9 N HCl,  $170\text{ }^{\circ}\text{C}$ , 40 min, microwave; (i) TFA,  $\text{CH}_2\text{Cl}_2$ ; (j)  $\text{CH}_2\text{O}$ ,  $\text{NaCNBH}_3$ .

basis of work from Christianson and others, we initiated a drug discovery program to identify novel potent arginase inhibitors that would be suitable for clinical development as treatments for myocardial ischemia/reperfusion injury (MI/RI). We directed our efforts to a structure-based design program using ABH as a starting template. After studying the arginase I binding interactions with the amino acid-based inhibitor, we rapidly identified the  $\alpha$ -position of the amino acid as an excellent site for novel substituents that could provide additional binding interactions with the protein.<sup>14</sup> In particular, Asp 181 and Asp 183 (ArgI) appeared to be ideally positioned to form new ionic interactions with the inhibitor to improve binding affinity. Herein we report our initial efforts to identify, prepare, and evaluate this new class of  $\alpha,\alpha$ -disubstituted amino acid-based arginase inhibitors, and the discovery of **9**, a novel second generation arginase inhibitor with significant activity in a rat model of MI/RI.

## INHIBITOR DESIGN AND SYNTHESIS

As we began investigating methods to prepare our  $\alpha,\alpha$ -disubstituted amino acid target compounds, we wanted to utilize a flexible late-stage intermediate that could be prepared on large research scale with very high enantioselectivity (>98% ee). We also wanted the ability to make either enantiomer and have the asymmetric center fixed in an early intermediate to simplify the synthesis and characterization of final compounds. After evaluating many approaches, we found the Williams' diphenyloxazinone to be a highly effective optically active glycine equivalent that could meet our needs. With our objective of identifying novel ABH analogues containing substituents in the  $\alpha$ -position to form new interactions with the Asp 181 and Asp 183 residues, we decided to pursue compounds with a substituted ethyl amine substituent. These compounds could be conveniently prepared from an intermediate aldehyde using a reductive amination reaction. This method was developed and is illustrated in Scheme 1.

Here, the syntheses of (*R*)-2-amino-6-borono-2-(2-(piperidin-1-yl)ethyl)hexanoic acid, **9**, and (*R*)-6-borono-2-(methyl-

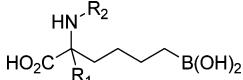
amino)-2-(2-(piperidin-1-yl)ethyl)hexanoic acid, **14**, are described to exemplify the general synthetic methods.

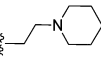
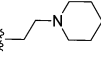
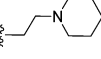
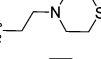
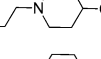
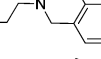
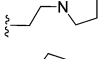
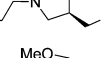
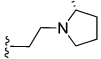
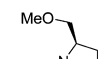
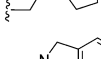
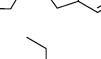
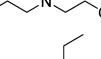
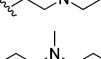
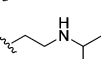
To obtain final compounds with the necessary configuration, we began with (*4S,5S*)-*tert*-butyl 6-oxo-4,5-diphenyl-1,3-oxazinane-3-carboxylate, **1**, which was prepared as described by Williams.<sup>15</sup> In an effort to make the synthesis more convergent, the protected butane boronic acid moiety was introduced in a single step via alkylation with (4-iodobutyl)boronic acid pinacol ester (**2**) using NaHMDS and HMPA in THF. Iodide **2** was prepared from 4-bromobutene in three steps: hydroboration with catechol borane followed by transesterification with pinacol and displacement of the bromide with sodium iodide in acetone (details in experimental section). Introduction of the second alkyl group to the oxazinone core proved challenging. Initial attempts with a variety of electrophiles (e.g., methyl iodide, benzyl iodide, and allyl iodide), using a variety of bases (LDA, KHMDS, LiHMDS, and NaH) in a variety of polar aprotic solvents (e.g., DMF, THF, DMA, and DMSO) with a variety of additives (including 18-crown-6, HMPA, and TMEDA) provided only modest yields and required many equivalents of base and electrophile. Eventually, we discovered that the use of dimethoxyethane (DME) as the solvent dramatically enhanced the reaction rate and that good electrophiles like allyl iodide could be introduced very effectively, even at  $-78\text{ }^{\circ}\text{C}$ . Although it is not entirely clear why this second alkylation was so difficult or why the use of DME resulted in such a dramatic acceleration of the reaction, it may be due, at least in part, to the boron atom in the side chain. Once the oxazinone moiety is deprotonated, a stable 6-membered boronate complex may be formed that effectively blocks the enolate from reaction with electrophiles. DME as a solvent may be more effective at preventing formation of this cyclic complex or reducing its stability.

Disubstituted oxazinone (**4**) and its enantiomer were prepared as common intermediates to provide access to target compounds with the necessary stereochemistry for activity (e.g., **9**) and their inactive enantiomers to serve as negative controls. To establish optical purity of compounds derived

from intermediate **4** or its enantiomer, compound **9** and its inactive enantiomer **15** (Table 1) were analyzed using a

**Table 1. Inhibition of Recombinant hARG I and hARG II Enzymes by Aminoethylene ABH Analogues**



Cmpd.	R <sub>1</sub>	R <sub>2</sub>	Absolute Configuration <sup>a</sup>	Inhibition (IC <sub>50</sub> ) <sup>b</sup>	
				hARG I	hARG II
ABH	H	H	R	1,450 nM	1,920 nM
9		H	R	223 nM	509 nM
14		CH <sub>3</sub>	R	60 nM	67 nM
15		H	S	> 300 μM	> 300 μM
16		H	R	1,240 nM	2,560 nM
17		H	R	230 nM	420 nM
18		H	R	510 nM	1,090 nM
19		H	R	160 nM	310 nM
20		H	R	260 nM	600 nM
21		H	R	210 nM	340 nM
22		H	R	1,750 nM	1,710 nM
23		H	R	270 nM	550 nM
24		H	R	550 nM	390 nM
25		H	R	270 nM	270 nM
26		H	R	140 nM	320 nM
27		H	R	100 nM	190 nM

<sup>a</sup>Stereochemistry of quaternary amino acid center. <sup>b</sup>Enzyme potency data is generated in triplicate. Compounds **9** and **14** were tested on multiple occasions. The combined data expressed as mean ± S.E.mean and number of experiments (in parentheses) for these compounds are as follows: compound **9**, Arg I IC<sub>50</sub> 223 ± 22.3<sup>9</sup> and Arg II IC<sub>50</sub> 509 ± 85.1;<sup>10</sup> and compound **14**, Arg I IC<sub>50</sub> 59.7 ± 9.1<sup>3</sup> and Arg II IC<sub>50</sub> 67 ± 13.3.<sup>3</sup>

Supelco Chirobiotic T2 analytical HPLC column and were found to have an optical purity of >98% ee (details provided as Supporting Information). Since all analogues were derived from the same intermediates and the quaternary chiral center is nonpimerizable, optical purity measurements of final compounds using chiral HPLC were not done on a routine basis. Several compounds, however, were prepared as both the active

and inactive enantiomers, and in all cases, the inactive compounds had no activity (<10% inhibition at 300 μM).

With the asymmetric center firmly established, the chiral auxiliary could be removed to facilitate new analogue synthesis. Treatment of oxazinone **4** with lithium in ammonia gave *N*-Boc protected amino acid **5**, which, after allowing the ammonia to evaporate, was redissolved in methanol and treated with TMS-diazomethane to provide methyl ester **6** in 58% yield (2 steps). Ozonolysis in dichloromethane followed by reduction of the ozonide with triphenylphosphine gave aldehyde **7**, which could be easily purified using column chromatography and was stable at room temperature for several days or could be stored in the refrigerator without significant decomposition for several months.

Aldehyde **7** was prepared in gram quantities and served as a key intermediate for new analogue synthesis. Reductive amination with piperidine and sodium triacetoxyborohydride in acetic acid-dichloromethane gave amine **8**, which was deprotected with 6 N HCl at 95 °C overnight to give target amino acid **9**. Although these compounds are very polar and have no chromophore, they could be conveniently purified using reverse phase preparative HPLC equipped with an ELSD detector (details in experimental section).

To facilitate a larger scale synthesis of compound **9** and other analogues, an alternative synthetic route was developed. As also illustrated in Scheme 1, oxazinone **4** could be subjected to the same ozonolysis and reductive amination conditions to provide amine **11** in 69% yield (2 steps). Subsequent cleavage of the chiral auxiliary via hydrogenolysis, however, proved to be exceedingly slow and required nearly stoichiometric palladium. Eventually, we developed a new method to remove the oxazinone auxiliary. Treatment with 9 N HCl in a microwave reactor for 40 min at 170 °C conveniently cleaved the auxiliary resulting in efficient formation of target amino acid **9** in 87% yield. On the basis of our experience, this method seems to be quite general and effective for acid and thermally stable oxazinones.

The *N*-methylated analogue **14** could also be prepared from oxazinone **11** as illustrated in Scheme 1. In this case, selective deprotection of the Boc-group with TFA in dichloromethane followed by reductive amination with formaldehyde using sodium cyanoborohydride gave *N*-methyl oxazinone **13** in 73% yield (2 steps). Final deprotection using the aforementioned microwave conditions provided the target *N*-methyl analogue, compound **14**, in 76% yield.

## RESULTS AND DISCUSSION

The primary objective of this program was to identify novel, highly potent and efficacious arginase inhibitors to treat individuals with MI/RI. All program compounds were initially tested for potency in human recombinant arginase I and II enzyme assays (hARG I and II), measuring the inhibition of arginase-induced urea production. Selected compounds were subsequently evaluated in a cellular functional assay with stably transfected human arginase I in CHO cells; the end point assessed was again inhibition of urea production. Results from these experiments are listed in Tables 1 and 2. A selected early compound, **9**, which was potent against hARG I in both in vitro enzyme and cellular assays, was selected for pharmacokinetic evaluation and subsequently was evaluated in a rat model of MI/RI. Results from these studies are provided in Table 3 and Figure 9.

**Table 2. Inhibitory Effects of Select Compounds in CHO Cells Over-Expressing hArgI**

example #	inhibition of CHO-hARG I (IC <sub>50</sub> )
9	8 $\mu$ M
14	3 $\mu$ M
15	inactive
ABH	19 $\mu$ M

**Table 3. Pharmacokinetic Profile of Compound 9 in Rat**

route dose (mg/kg)	i.v. 10	p.o. 10
AUC <sub>0-inf</sub> (mg-h/L)	21.2	5.92
C <sub>0</sub> or C <sub>max</sub> (mg/L)	40.3	0.45
t <sub>1/2</sub> (h)	3.30	n/a
CL (mL/min/kg)	7.89	n/a
V <sub>ss</sub> (L/kg)	1.86	n/a
F (%)	n/a	28%

The use of X-ray crystallography early in the program was essential. The structures provided a clear understanding of the important interactions that make up the enzyme–inhibitor complexes. An iterative structure based design approach was then used to drive analogue synthesis, focused on introducing new interactions with residues at the mouth of the active site pocket, particularly with Asp 181 and Asp 183.

In general, the structure–activity relationships associated with the compound class (Table 1) are consistent with binding information derived from the enzyme–inhibitor complexes. In compound 9, the  $\alpha$  substituent, which consists of a piperidine linked to the  $\alpha$  carbon by a two-carbon aliphatic chain, results in formation of new through-water hydrogen bonding interactions with Asp 181 and Asp 183 and provides a 6-fold increase in potency relative to ABH. The magnitude of this improvement decreases when larger substituents force the side chain amine into a conformation where the interactions between the basic amine and carboxylate of Asp 181 and Asp 183 are suboptimal. Figure 1 shows the binding of compound 9 to the active site pocket of arginase I and the corresponding electron density. Two alternative conformations are observed for the piperidine ring: a distorted boat (major occupancy) and a chair (minor occupancy). While in the distorted boat conformation, the amine nitrogen forms hydrogen bonding interactions through water molecule W1 with Asp 181 (3.10 Å) and Asp 183 (3.70 Å) (Figure 3). In the chair conformation, amine nitrogen is pointing toward the solvent and does not have strong contacts with the protein (Figure 1). Moreover, the minor chair conformation of the piperidine ring (in gold) places the piperidine C1 atom of 9 in a position that is too close to water molecule W1 (1.89 Å, Figure 2), implying that W1 is not present in the population of molecules containing the chair conformer. Therefore, the water-mediated contacts with Asp 181 and Asp 183 likely do not exist for the chair conformation, which may explain its lower occupancy despite the fact that it is the more thermodynamically stable conformer.

Like ABH, the amino acid and boronic acid moieties form multiple hydrogen bonding or ionic interactions that hold the inhibitor securely within the active site. Figure 3 shows the contacts between the protein, the Mn ions, and the major boat conformation of 9. Amine N1 (amino acid amine) of the inhibitor forms a direct contact with Asp 183 (2.91 Å) and water mediated contacts with Glu 186 and Gly 142 through water molecule W3 (3.0 Å), and with Asp 181 through W2

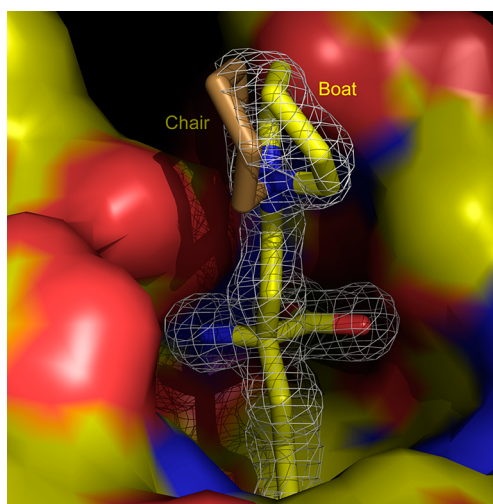


**Figure 1.** Structure of compound 9 (stick model) in the active site pocket of arginase I (surface colored according to charge), is shown superimposed with a difference map calculated without the inhibitor model contoured at 3 RMS (white contours). Note that the map shows very clearly the inhibitor structure and indicates that the piperidine ring has two conformations, a major one (yellow sticks, occupancy 0.66, ring in distorted boat conformation) and a minor one (gold sticks, occupancy 0.33, ring in chair conformation).

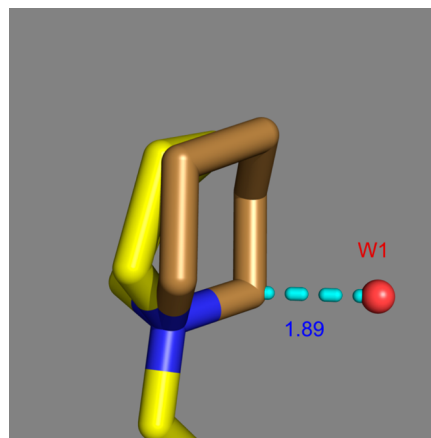


**Figure 2.** Minor chair conformation of the piperidine ring (in gold) where the inordinately short distance between the piperidine C1 atom (1.89 Å) and W1 implies that W1 is not present in this conformation in the arginase I: compound 9 complex.

(2.66 Å). The carboxylic acid forms direct interactions with Ser 137 (OH, 2.57 Å) and Asn 130 (3.14 Å) and hydrogen bonding interactions (through three water molecules) with Thr 135 (2.91 Å), Asn 139 (2.99 Å), and Asp 183 (2.72 Å) (Figure 4).

The butylboronic acid chain of the inhibitor is buried in the active site cleft and makes contacts similar to those of ABH. The oxygen atoms linked to the boron form close contacts with the arginase Mn ions, and these substituents are surrounded by aspartic acid residues Asp 128 (2.63 Å) and Asp 232 (3.14 Å) (Figure 3).

Because of the many important protein interactions with the amino acid amine N1, only limited modifications are possible. Interestingly, as seen with compound 14, incorporation of a simple methyl substituent at position R1 results in a nearly 4-fold increase in potency. As illustrated in Figure 5, the binding mode is very similar to that of compound 9, except the

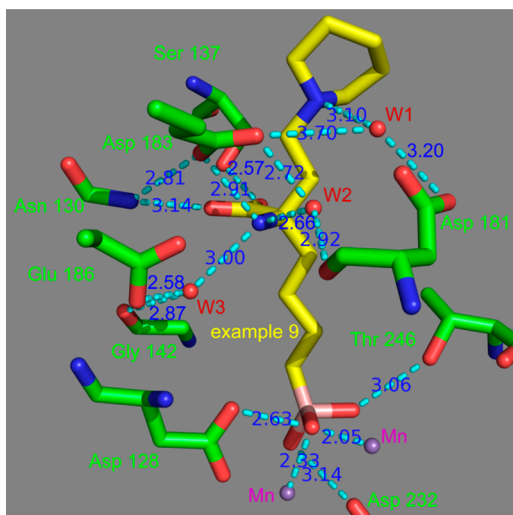


**Figure 3.** Contacts of compound **9** with the arginase I and the Mn atoms in the major conformation (distorted boat).

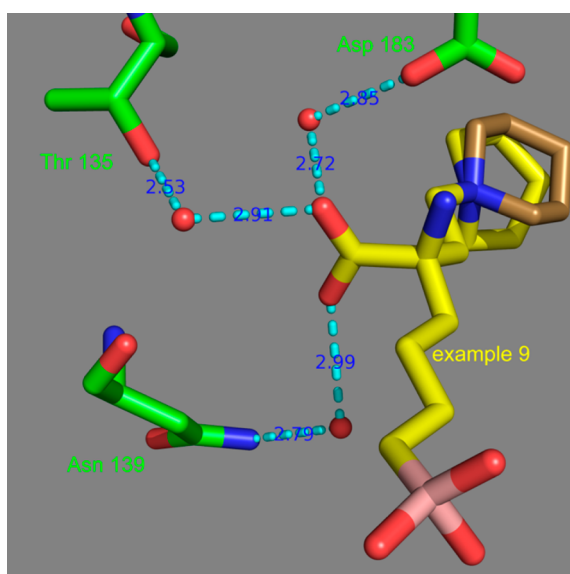


**Figure 4.** Contacts of the carboxylic acids, Asn 139, Thr 135, and Asp 183, in the arginase I: compound **9** complex.

orientation of the piperidine ring resides exclusively in the more thermodynamically stable chair conformation.

As expected, the contacts for compound **14** (Figure 6) are very similar to those of compound **9**. In each case, the inhibitor forms an almost identical network of hydrogen bonding interactions with the key active site amino acids and waters W1 and W3. The major difference is that water molecule W2 is ejected by the methyl group. Although this results in the loss of W2 hydrogen bonding interactions, the increased potency (lower  $IC_{50}$ ) for compound **14** (60 nM for compound **14** versus 223 nM for compound **9**) implies a net increase in binding energy. This probably results from a gain in entropy due to the liberation of water molecule W2 and the strengthening of existing hydrogen bonds made possible by minor conformational changes of the inhibitor and active site amino acid side chains.

Example **9** was also cocrystallized with arginase II (see details in Supporting Information). The two structures are very similar; in particular, the through-water contacts between the

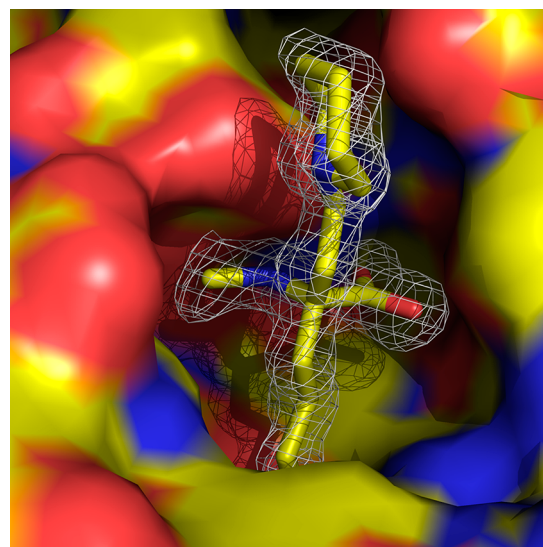


**Figure 5.** Contacts of compound **14** (stick model) within the active site pocket of arginase I (surface colored according to charge), superimposed with a difference map calculated without the inhibitor model contoured at 3 RMS (white contours). Note that the map shows very clearly the inhibitor structure and that the piperidine ring adopts only the chair conformation.

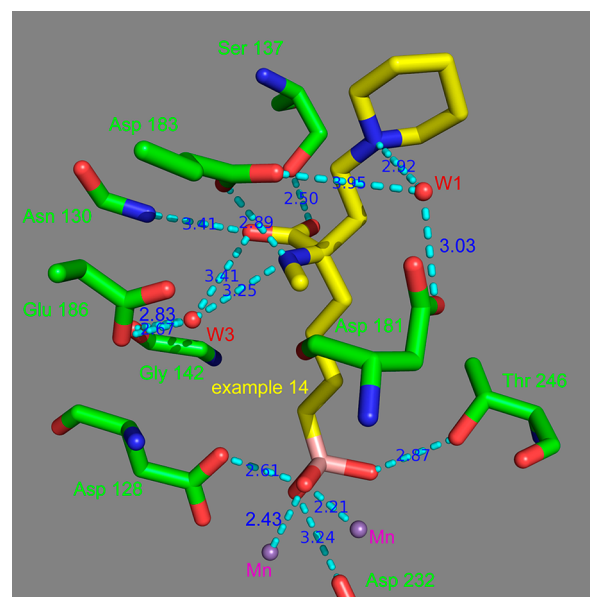


**Figure 6.** Contacts of compound **14** with the arginase I and Mn atoms.

piperidine ring nitrogen atom and the aspartic acid residues (181 and 183 in arginase I; 200 and 202 in arginase II) are maintained.

As shown in Figure 7, for the arginase II complex, the piperidine ring (contacting both aspartic acid residues) is in the chair conformation, and one of the distances, between water molecule W1 and Asp 202 (4.27 Å), is beyond hydrogen bond range, while it can make a weak hydrogen bond (3.95 Å) in the arginase I complex. This difference may partially explain the weaker binding of compound **9** to arginase II ( $IC_{50}$  509 nM) relative to arginase I ( $IC_{50}$  223 nM).

We have also solved the complex of arginase II cocrystallized with compound **14** (see Supporting Information). In this case, the inhibitor positions are very close for both Arg I and Arg II

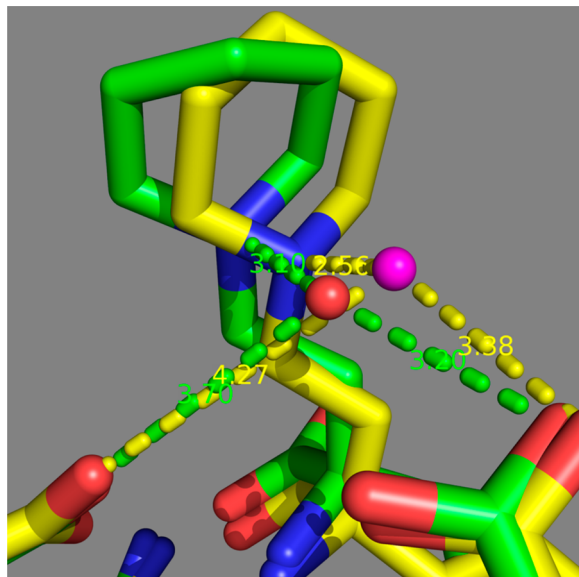


**Figure 7.** Superimposition of the arginase I–compound 9 complex (green carbons, red water W1, and green distances) and the arginase II–compound 9 complex (yellow carbons, magenta water W1, and yellow distances).

(see Figure 8). For these compounds, the distances between the water molecule W1 and the aspartic acids are all within

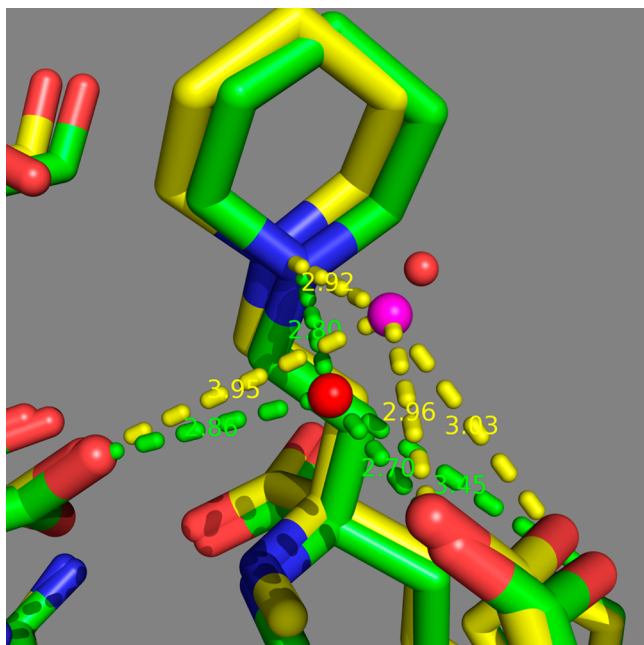


**Figure 8.** Superimposition of the arginase I–compound 14 complex (green carbons, red water W1, and green distances) and the arginase II–compound 14 complex (yellow carbons, magenta water W1, and yellow distances).

hydrogen bonding range (Figure 8). This is consistent with the statistically equivalent  $IC_{50}$  values for Arg I and Arg II (60 nM and 67 nM, respectively).

As expected, the small, highly polar enzyme active site accommodates only amino acids with the natural R-stereo configuration. Unnatural amino acids with the S-configuration like compound 15 are completely inactive with <10% inhibition

at 300  $\mu$ M. Modification of the piperidine ring generally did not result in improved potency. Analogues with a sulfur atom (16), a 4'-hydroxyl substituent (17), or a benzo-moiety (18) were all less active. Similar results were observed with the pyrrolidine series. The addition of a hydroxymethyl (20) or methoxymethyl substituent (21, 22) to the parent pyrrolidine (19) also did not improve potency. It is interesting to note the difference in activity between the analogues with the methoxymethyl substituents in the R- and S-configurations. In compound 21 (R-stereochemistry), the ether oxygen is able to form an additional weak hydrogen bonding interaction with Ser 155 (OH, 3.78 Å, structural data not shown). This likely contributes to the increased potency observed for compound 21 relative to compound 22. Benzo-modification of the pyrrolidine side chain (23) results in about a 2-fold decrease in potency relative to the unsubstituted compound (19). This is consistent with what is observed for the piperidines (compounds 9 and 18). Potency for compounds 24–27, with acyclic side chains (ethyl, hydroxyethyl; diethyl; methyl, propyl; or methyl, isopropyl) varied depending on the size of the amine substituents. Those with a small substituent (methyl 26 or hydrogen 27) were more potent than those with two larger substituents (24 and 25). This presumably results from a more optimal binding interaction with Asp 181 and Asp 183 when the amine is less sterically hindered.

To better characterize these compounds as arginase inhibitors, they were evaluated in a cellular functional assay with stably transfected human arginase I in CHO cells. As illustrated in Table 2, the rank-order potencies for compounds 9 and 14 and ABH observed in the cell assay are consistent with those obtained in the recombinant hARG I enzyme assay (Table 1). The  $IC_{50}$  values for compounds 9 and 14 are 8 and 3  $\mu$ M, respectively, each about 50-fold less active than that observed in the isolated enzyme assay. For example, 15, the inactive enantiomer of 9, was completely inactive in the cellular assay. ABH has an  $IC_{50}$  of 19  $\mu$ M in this assay. The differences in activity between the isolated enzyme assay and the cellular assay is not fully understood at present. Presumably, the charged polar nature of these compounds precludes passive diffusion through the cell membrane and an active transport mechanism may be involved. Further work is required to investigate the mechanism of cellular absorption.

A pharmacokinetic evaluation of compound 9 was conducted after intravenous (i.v.) and oral (p.o.) dosing in male Sprague–Dawley rats ( $n = 3$  per dose route). The compound was formulated in 0.9% saline and administered intravenously at 10 mg/kg by bolus through a preimplanted cannula at a dosing volume of 1 mL/kg, and orally at 10 mg/kg via gavage at a dosing volume of 2 mL/kg. As illustrated in Table 3, following i.v. dosing with 10 mg/kg in fasted animals, compound 9 has a terminal elimination half-life ( $t_{1/2}$ ) of 3.3 h with a volume of distribution and total body clearance of 1.86 L/kg and 7.89 mL/min/kg, respectively. The oral bioavailability of compound 9 (10 mg/kg, p.o.) was 28% with a  $C_{max}$  of 0.45 mg/L.

To determine if arginase inhibition following myocardial ischemia/reperfusion injury (MI/RI) would limit tissue damage, compound 9 and its inactive enantiomer 15 were evaluated in a rodent model of MI/RI, involving occlusion of the left-main coronary artery for 45 min. Also included in the study were sham (no occlusion), vehicle (occlusion, no drug), and groups receiving intermittent preconditioning (IPC) as a positive control. The IPC group was implemented as 3  $\times$  5 min of intermittent occlusion prior to the 45 min of sustained

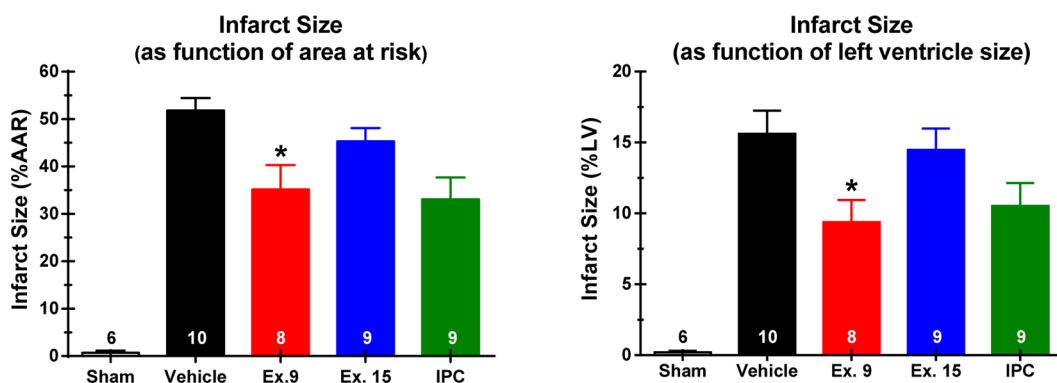


**Figure 9.** Effect of compounds **9** and **15** on infarct size expressed as a percent of the area at risk (AAR; left panel) and percent of the left ventricle (right panel) 2 days postreperfusion in a rat model of MI/RI. Compounds **9** (100 mg/kg, i.v.) and **15** (100 mg/kg, i.v.) were given as bolus administration 15 min before occlusion of the left main coronary artery. Intermittent preconditioning (IPC) was implemented as 3 × 5 min of intermittent occlusion prior to the 45 min sustained ischemia. \**p* < 0.05 vs vehicle; the *n* values for each group are indicated in the individual columns.

ischemia. After 2 days, infarct size was measured and expressed as a percent of the area at risk (AAR) and as a function of left ventricle size. Results of the study are illustrated in Figure 9. Infarct size in the control group averaged 51.8% of the AAR, while IPC produced a reduction of infarct size to 33.1% of the AAR. Treatment with compound **9** (100 mg/kg, i.v.) reduced infarct size to 35.2% of AAR, similar to the IPC group, while using compound **15**, the inactive enantiomer of compound **9**, had no effect on infarct size.

In conclusion, a novel second generation series of  $\alpha,\alpha$ -disubstituted amino acid ABH analogues has been identified and optimized to be highly potent inhibitors of both human arginase I and II. Significant improvements in potency were achieved by introducing an aminoethylene substituent to form new hydrogen bonding interactions with Asp 181 and Asp 183 near the mouth of the active site. In vivo evaluation of compound **9**, (*R*)-2-amino-6-borono-2-(2-(piperidin-1-yl)ethyl)hexanoic acid, in a rat model of MI/RI resulted in a significant reduction in infarct size, which was similar to the IPC. Continued development of this new class of compounds may result in an important new treatment for ischemia reperfusion injury.

Samples of compounds **9** and **15** will be provided, when possible, to facilitate further preclinical research into the role of arginases in MI/RI and other relevant diseases. Please contact the corresponding author for details.

## EXPERIMENTAL SECTION

**Chemistry. General Methods.** Melting points were determined in open capillary tubes on a Thomas-Hoover apparatus and are uncorrected. Proton nuclear magnetic resonance ( $^1\text{H}$  NMR) spectra were determined on a Bruker Avance III 400 MHz NMR spectrometer. Chemical shifts are provided in parts per million (ppm) downfield from tetramethylsilane (internal standard) with coupling constants in hertz (Hz). Multiplicity is indicated by the following abbreviations: singlet (s), doublet (d), triplet (t), quartet (q), multiplet (m), and broad (br). Mass spectra were recorded on a PE Sciex API 100 LC/MS system equipped with a Perkin-Elmer 200 Series autosampler and LC pump. Elemental analyses (C, H, N, S, Cl, and Br) were performed by Atlantic Microlab, Inc. (Norcross, Georgia) and are within  $\pm 0.4\%$  of theory unless otherwise noted. Intermediate products from all reactions (nonpolar compounds) were purified by either flash column chromatography or medium pressure liquid chromatography using a Biotage Isolera One with SNAP cartridges unless otherwise indicated. All final products were purified

on a Gilson preparative LC system consisting of a robotic liquid handler 215, a syringe pump 402, an injection module 845z, and a binary pump 322, using a Phenomenex C18 amino acid preparative column with a Gilson ELSD detector. Using these methods, purity was determined to be >95% except where noted. Analytical data for all compounds is provided as Supporting Information. Thin-layer chromatography using glass-backed silica plates containing a fluorescent indicator (0.25 mm, Whatman, Merck) was used to monitor reactions. The chromatograms were visualized using ultraviolet illumination, exposure to iodine vapors, or dipped in an aqueous potassium permanganate solution. All starting materials were used without further purification. All reactions were carried out under an atmosphere of dried nitrogen or argon. Compound names are based on IUPAC convention and are derived from the structures using ChemDraw Ultra 12.0.

**General Procedures for the Synthesis of Substituted 2-Amino-2-(2-aminoethyl)-6-boronohexanoic Acids.** The 2-amino-2-(2-aminoethyl)-6-boronohexanoic acids in Table 1 were prepared from (4*S*,5*S*)-*tert*-butyl-6-oxo-4,5-diphenyl-1,3-oxazinane-3-carboxylate **1** or its enantiomer (compound **15**) and 2-(4-iodobutyl)-4,4,5,5-tetramethyl-1,3,2-dioxaborolane (**2**) as outlined in Scheme 1 via the general methods described for compounds **9** and **14** below. (4*S*,5*S*)-*tert*-Butyl-6-oxo-4,5-diphenyl-1,3-oxazinane-3-carboxylate (**1**) and its enantiomer were prepared according to the methods described by Williams.<sup>15</sup>

**Synthesis of 2-(4-Iodobutyl)-4,4,5,5-tetramethyl-1,3,2-dioxaborolane (**2**).** **Step 1: Synthesis of 2-(4-Bromobutyl)-4,4,5,5-tetramethyl-1,3,2-dioxaborolane.** While under nitrogen, neat catecholborane (100 g, 833 mmol) in a 1 L round-bottomed flask was cooled in an ice bath and carefully treated with 4-bromobutene (124.2 g, 920 mmol) via syringe at a rate such that the temperature remained below 20 °C. After the addition was complete, the ice bath was removed, and the solution was allowed to warm to room temperature over 30 min, then warmed to 95 °C for 6 h. After recooling to room temperature, the reaction mixture was diluted with anhydrous THF (300 mL), treated with pinacol (217.5 g, 1.84 mol) in one portion, and stirred for an additional 16 h, while still under a nitrogen atmosphere. The resulting solution was concentrated to give the crude product as a pale yellow oil that was diluted with heptane (800 mL) and cooled to -40 °C in a dry ice/acetone bath. After stirring for 1 h, the precipitated catechol and excess pinacol were removed by filtration to give 2-(4-bromobutyl)-4,4,5,5-tetramethyl-1,3,2-dioxaborolane as a colorless oil (195 g, 89%), which generally contained 2–6% free catechol (this material could be further purified by repeated precipitation from chilled heptane, although this level of catechol contamination was not detrimental to the subsequent step);  $^1\text{H}$  NMR ( $\text{CDCl}_3$ , 400 MHz)  $\delta$  3.38 (t, *J* = 6.6 Hz, 2 H), 1.90–1.78 (m, 2 H), 1.58–1.44 (m, 2 H), 1.26 (s, 12 H), 0.78 (t, *J* = 7.5 Hz, 2 H).

**Step 2: Synthesis of 2-(4-Iodobutyl)-4,4,5,5-tetramethyl-1,3,2-dioxaborolane (**2**).** While under a nitrogen atmosphere, a solution of

crude 2-(4-bromobutyl)-4,4,5,5-tetramethyl-1,3,2-dioxaborolane (195 g, 0.741 mol) and sodium iodide (333.6 g, 2.24 mol) in acetone (500 mL) was heated to 55 °C overnight. After cooling to room temperature, the solution was concentrated, diluted with heptane (1 L), cooled to 0 °C with stirring for 30 min, and filtered. The filtrate was concentrated to give 2-(4-iodobutyl)-4,4,5,5-tetramethyl-1,3,2-dioxaborolane (2) as a colorless oil (189 g, 83%). <sup>1</sup>H NMR (CDCl<sub>3</sub>, 400 MHz) δ 3.18 (t, J = 7.2 Hz, 2 H), 1.90–1.78 (m, 2 H), 1.58–1.44 (m, 2 H), 1.24 (s, 12 H), 0.79 (t, J = 7.5 Hz, 2 H).

**Large Scale Synthesis of (R)-2-Amino-6-borono-2-[2-piperidin-1-yl]ethyl-hexanoic Acid (9).** **Step 1: Synthesis of (3R,5R,6S)-tert-Butyl 2-Oxo-5,6-diphenyl-3-(4-(4,4,5,5-tetramethyl-1,3,2-dioxaborolan-2-yl)butyl)morpholine-4-carboxylate (3).** A solution of (2S,3R)-tert-butyl-6-oxo-2,3-diphenylmorpholine-4-carboxylate (1, 68.0 g, 192.8 mmol) and 2-(4-iodobutyl)-4,4,5,5-tetramethyl-1,3,2-dioxaborolane (2, 74.7 g, 241.0 mmol, 1.25 equiv) in THF (1000 mL) and HMPA (100 mL) was cooled to –78 °C and treated with sodium bis(trimethylsilyl)amide (250.6 mL, 1.0 M, 250.6 mmol) dropwise over 60 min. After stirring for 2 h at –78 °C, the solution was warmed to 0 °C with stirring for an additional 4 h and then warmed slowly to room temperature overnight. The solution was diluted with ethyl acetate (1000 mL) and quenched with saturated aqueous NH<sub>4</sub>Cl. The organic solution was washed successively with water and saturated aqueous sodium chloride, dried over anhydrous MgSO<sub>4</sub>, filtered, and concentrated to give the product as a sticky white gum. Heptane (800 mL) was added, and the slurry was stirred at room temperature for 2 h to precipitate the product. The product was vacuum filtered to give a white solid that was dried in a vacuum desiccator overnight, to afford (3R,5R,6S)-tert-butyl-2-oxo-5,6-diphenyl-3-(4-(4,4,5,5-tetramethyl-1,3,2-dioxaborolan-2-yl)butyl)morpholine-4-carboxylate (3) as a white solid (85.8 g, 83%). [ $\alpha$ ]<sub>D</sub><sup>25</sup> +39.64° (c 3.91, CHCl<sub>3</sub>); <sup>1</sup>H NMR (CDCl<sub>3</sub>, 400 MHz) δ 7.25 (m, 3 H), 7.12 (m, 1 H), 7.06 (m, 2 H), 6.98 (m, 2 H), 6.57 (t, J = 7.5 Hz, 2 H), 5.93 (d, J = 3 Hz, 1 H), 5.20 and 4.99 (d, J = 3 Hz, ~ 1:2 rotamers, combined 1 H), 5.01 and 4.81 (dd, J<sub>1</sub> = 10.5, J<sub>2</sub> = 4.5 Hz, ~ 1:2 rotamers, combined 1 H) 2.15 (m, 1 H), 1.98 (m, 1 H), 1.52–1.66 (m, 4 H), [1.44 (s, 3 H) and 1.08 (s, 6 H); ~ 1:2 Boc rotamers], 1.24 (s, 12 H) 0.85 (m, 2 H); LC-MS 558.3 (M + Na)<sup>+</sup>, 536.3 (M + H)<sup>+</sup>, 480.3 (M + H-iBu)<sup>+</sup>, 436.2 (M + H-Boc)<sup>+</sup>; Anal. Calcd for C<sub>31</sub>H<sub>42</sub>BNO<sub>6</sub>, C, 69.53; H, 7.91; N, 2.62. Found C, 69.36; H, 7.80; N, 2.55.

**Step 2: Synthesis of (3R,5R,6S)-tert-Butyl 3-Allyl-2-oxo-5,6-diphenyl-3-(4-(4,4,5,5-tetramethyl-1,3,2-dioxaborolan-2-yl)butyl)morpholine-4-carboxylate (4).** A solution of (3R,5R,6S)-tert-butyl-2-oxo-5,6-diphenyl-3-(4-(4,4,5,5-tetramethyl-1,3,2-dioxaborolan-2-yl)butyl)morpholine-4-carboxylate (3, 70.0 g, 123.2 mmol) and TMEDA (100 mL) in DME (1,200 mL) was cooled to –78 °C, charged with allyl iodide (310.5 g, 1.85 mol, 15 equiv), and treated with potassium bis(trimethylsilyl)amide (962 mL, 1.0 M in THF, 862 mmol, 7 equiv) dropwise over 60 min. After stirring for 2 h, a second portion of allyl iodide (150 g, 0.89 mol) was added, followed by the dropwise addition of additional KHMDS (400 mL, 1.0 M in THF). After stirring an additional 3 h at –78 °C, the reaction mixture was slowly warmed to room temperature overnight. Once complete as indicated by thin-layer chromatography, the reaction mixture was quenched with saturated aqueous sodium chloride and extracted with diethyl ether (3 × 1.5 L). The combined organic phase was washed successively with water and saturated aqueous NH<sub>4</sub>Cl, dried over anhydrous MgSO<sub>4</sub>, filtered, and concentrated. Purification by suction filtration through silica gel (0–20% ethyl acetate in heptane) gave (3R,5R,6S)-tert-butyl-3-allyl-2-oxo-5,6-diphenyl-3-(4-(4,4,5,5-tetramethyl-1,3,2-dioxaborolan-2-yl)butyl)morpholine-4-carboxylate as a pale yellow oil (4, 65.5 g, 92.5%). [ $\alpha$ ]<sub>D</sub><sup>25</sup> –43.13° (c 6.38, CHCl<sub>3</sub>); <sup>1</sup>H NMR (CDCl<sub>3</sub>, 400 MHz) δ 7.02–7.18 (m, 11 H), 6.09 (d, J = 3 Hz, 1 H), 5.86 (m, 1 H), 5.22 (m, 2 H), 3.21 (m, 1 H), 2.84 (m, 1 H), 2.17 (m, 2 H), 1.52 (s, 9 H), 1.10–1.45 (m, 9 H), 1.18 (s, 12 H), 0.48 (t, J = 7 Hz, 2H); LC-MS 598.3 (M + Na)<sup>+</sup>, 576.3 (M + H)<sup>+</sup>, 510.3 (M + H-iBu)<sup>+</sup>, 476.3 (M + H-Boc)<sup>+</sup>; Anal. Calcd for C<sub>34</sub>H<sub>46</sub>BNO<sub>6</sub>, C, 70.95; H, 8.06; N, 2.43. Found C, 71.02; H, 8.27; N, 2.55.

**Step 3: Synthesis of (3R,5R,6S)-tert-Butyl 2-Oxo-3-(2-oxoethyl)-5,6-diphenyl-3-(4-(4,4,5,5-tetramethyl-1,3,2-dioxaborolan-2-yl)-**

**butyl)morpholine-4-carboxylate (10).** A solution of (3R,5R,6S)-tert-butyl-3-allyl-2-oxo-5,6-diphenyl-3-(4-(4,4,5,5-tetramethyl-1,3,2-dioxaborolan-2-yl)butyl)morpholine-4-carboxylate (4, 65.0 g, 113 mmol) in DCM (400 mL) was cooled to –78 °C and treated with ozone until a pale blue–gray color persisted. After thin-layer chromatography indicated the absence of starting material, the ozone inlet tube was replaced with a nitrogen inlet tube, and nitrogen was bubbled through the solution for 20 min to remove any excess ozone. Triphenylphosphine (44.5 g, 169.5 mmol) was added in one portion, the cooling bath was removed, and the mixture was stirred for 16 h. The resulting solution was concentrated and purified by suction filtration through a short pad of silica gel (10–50% ethyl acetate in heptane) to give (3R,5R,6S)-tert-butyl-2-oxo-3-(2-oxoethyl)-5,6-diphenyl-3-(4-(4,4,5,5-tetramethyl-1,3,2-dioxaborolan-2-yl)butyl)morpholine-4-carboxylate, 10, as a colorless foam (48.1 g, 73%), which was used without further purification. [ $\alpha$ ]<sub>D</sub><sup>25</sup> –60.21° (c 7.23, CHCl<sub>3</sub>); <sup>1</sup>H NMR (CDCl<sub>3</sub>, 400 MHz) δ 9.91 (s, 1 H), 7.49–7.27 (m, 10 H), 7.18 (s, 1 H), 6.35 (s, 1 H), 3.25 (d, J = 1.3 Hz, 1 H), 2.20 (br s, 1 H), 1.93 (br s, 1 H), 1.55 (m, 1 H), 1.50 (s, 9 H), 1.14 (s, 12 H), 1.03 (m, 2 H), 0.97 (m, 2 H), 0.68 (t, J = 7.6 Hz, 2 H); LC-MS 578.3 (M + H)<sup>+</sup>, 522.2 (M + H-iBu)<sup>+</sup>, 478.2 (M + H-Boc)<sup>+</sup>; Anal. Calcd for C<sub>33</sub>H<sub>44</sub>BNO<sub>7</sub>, C, 68.63; H, 7.68; N, 2.43. Found C, 68.53; H, 7.64; N, 2.42.

**Step 4: Synthesis of (3R,5R,6S)-tert-Butyl 2-Oxo-5,6-diphenyl-3-(2-(piperidin-1-yl)ethyl)-3-(4-(4,4,5,5-tetramethyl-1,3,2-dioxaborolan-2-yl)butyl)morpholine-4-carboxylate (11).** A solution of aldehyde 10 (38.0 g, 65.86 mmol) and piperidine (13.15 mL, 131.7 mmol) in 1,2-dichloroethane (250 mL) and acetic acid (7.8 mL, 131.7 mmol) was stirred at room temperature for 60 min and then treated with sodium triacetoxycoborohydride (34.91 g, 164.65 mmol) in 4 portions. After stirring for 16 h at room temperature, saturated aqueous NaHCO<sub>3</sub> was added until the solution reached pH 8–9, and stirring was continued for an additional 5 min. The resulting mixture was added to a separatory funnel, diluted with saturated aqueous sodium chloride (50 mL), and extracted with DCM (3 × 250 mL). The organic layer was dried over anhydrous MgSO<sub>4</sub>, filtered, and concentrated under reduced pressure. Purification by flash column chromatography, eluting with 30–100% ethyl acetate in heptane (+0.5% NEt<sub>3</sub>), gave a ~ 20:1 mixture of (3R,5R,6S)-tert-butyl-2-oxo-5,6-diphenyl-3-(2-(piperidin-1-yl)ethyl)-3-(4-(4,4,5,5-tetramethyl-1,3,2-dioxaborolan-2-yl)butyl)morpholine-4-carboxylate (LC-MS 647.3 (M + H)<sup>+</sup>, 591.2 (M + H-iBu)<sup>+</sup>, 547.2 (M + H-Boc)<sup>+</sup>) and (3R,5R,6S)-4-(tert-butoxycarbonyl)-2-oxo-5,6-diphenyl-3-(2-(piperidin-1-yl)ethyl)morpholin-3-yl)butyl boronic acid (formed by silica-promoted deprotection of the pinacol protecting group) as a colorless foam (40.3 g, 95%). [ $\alpha$ ]<sub>D</sub><sup>25</sup> –32.4° (c 8.81, CHCl<sub>3</sub>); <sup>1</sup>H NMR (CDCl<sub>3</sub>, 400 MHz) δ 7.41–7.20 (m, 10 H), 7.18 (s, 1 H), 6.22 (s, 1 H), 2.60–2.09 (m, 6 H), 2.06 (m, 1 H), 1.52 (s, 9 H), 1.52–1.30 (m, 7 H), 1.10 (s, 12 H), 1.10–0.96 (m, 4 H), 0.78 (m, 2 H), 0.72 (m, 2 H); LC-MS 565.3 (M + H)<sup>+</sup>, 509.2 (M + H-iBu)<sup>+</sup>, 465.2 (M + H-Boc)<sup>+</sup>. This mixture could be used in the subsequent deprotection steps, without separation of the boronic acid from the boronate.

**Step 5: Synthesis of (R)-2-Amino-6-borono-2-(2-(piperidin-1-yl)ethyl)hexanoic Acid (9).** A solution of (3R,5R,6S)-tert-butyl-2-oxo-5,6-diphenyl-3-(2-(piperidin-1-yl)ethyl)-3-(4-(4,4,5,5-tetramethyl-1,3,2-dioxaborolan-2-yl)butyl)morpholine-4-carboxylate 11 (40.3 g) in 6 N hydrochloric acid (300 mL) and acetic acid (20 mL) was warmed to 70 °C with stirring overnight. After cooling to room temperature, the reaction mixture was transferred to a separatory funnel, diluted with deionized water (50 mL), and washed with DCM (3×). The aqueous layer was concentrated to give the crude boronic acid intermediate as a white foam (34.2 g) that was redissolved in 9 N hydrochloric acid (200 mL) and transferred into 20 mL Biotage microwave reactor vials (20 tubes). The vials were capped and then heated, with stirring, in a Biotage Initiator microwave reactor to 170 °C for 40 min. After all 20 vials had been processed, the combined aqueous phase was washed with DCM (2 × 50 mL) and concentrated to give (R)-2-amino-6-borono-2-(2-(piperidin-1-yl)ethyl)hexanoic acid, dihydrochloride monohydrate salt as a very hygroscopic white foam (24.1 g). <sup>1</sup>H NMR (D<sub>2</sub>O, 300 MHz) δ 3.34 (d, J = 11.5 Hz, 2 H), 3.14 (m, 1 H), 2.97 (m, 1 H), 2.77 (t, J = 12 Hz, 2 H), 2.19 (t, J = 8.5 Hz, 2



H), 1.76 (m, 4 H), 1.55 (m, 3 H), 1.23 (m, 4 H), 1.06 (m, 1 H), 0.59 (t,  $J = 7.5$  Hz, 2 H); LC-MS 287.2 (M + H)<sup>+</sup>, 269.3 (M + H-H<sub>2</sub>O)<sup>+</sup>, 251.4 (M + H-2H<sub>2</sub>O)<sup>+</sup>; Anal. Calcd for C<sub>15</sub>H<sub>33</sub>BN<sub>2</sub>O<sub>4</sub>·2HCl, 1.25 H<sub>2</sub>O salt, expected C 40.92, H 8.32, Cl 18.58, N 7.34; measured C 40.90, H 7.95, Cl 18.45, N 6.97.

Dowex-50WX8-400 ion resin (Aldrich cat# 217514, 600 g) was washed by stirring successively with MeOH (2×) and water (2×), then briefly suction dried. The crude amino acid was dissolved in water (100 mL) and stirred with the resin at room temperature for 2 h (until LC-MS analysis of the aqueous phase failed to detect the amino acid MH<sup>+</sup> ion). The resin was filtered and then transferred to a sintered chromatography column. Water (~300 mL) was run through the resin column until an aliquot of the collected water fraction failed to give a positive AgNO<sub>3</sub> test (i.e., once all of the chloride had been successfully eluted from the column).

The salt-free amino acid was then recovered from the resin by eluting with aqueous 4 N NH<sub>4</sub>OH solution. Fractions were collected until the aqueous solutions were negative for ninhydrin staining and showed no MH<sup>+</sup> ion in LC-MS analysis. The combined product-containing fractions were concentrated to give (R)-2-amino-6-borono-2-(2-(piperidin-1-yl)ethyl)hexanoic acid (**9**) as a nonhygroscopic free base hydrate (17.9 g, 87% from **11**). [ $\alpha$ ]<sub>D</sub> +15.4° (c 2.27, H<sub>2</sub>O); <sup>1</sup>H NMR (D<sub>2</sub>O, 400 MHz)  $\delta$  2.84–3.05 (m, 6 H), 1.89 (m, 2 H), 1.68 (br s, 5 H), 1.51 (m, 3 H), 1.31 (m, 3 H), 1.08 (m, 1 H), 0.70 (t,  $J = 7.0$  Hz, 2 H); <sup>13</sup>C NMR (D<sub>2</sub>O, 400 MHz)  $\delta$  180.04, 62.22, 53.99, 53.20 (2× C), 38.98, 32.13, 25.86, 23.85, 23.53 (2× C), 21.72, 14.18; <sup>11</sup>B-NMR (D<sub>2</sub>O, 400 MHz) singlet at  $\delta$  32.55; LC-MS 309.4 (M + Na)<sup>+</sup>, 287.3 (M + H)<sup>+</sup>, 269.2 (M + H-H<sub>2</sub>O)<sup>+</sup>, 251.1 (M + H-2H<sub>2</sub>O)<sup>+</sup>; Anal. Calcd for C<sub>15</sub>H<sub>33</sub>BN<sub>2</sub>O<sub>4</sub>·1.5 H<sub>2</sub>O salt, expected C 49.85, H 9.65, Cl 0.00, N 8.94; measured C 49.95, H 9.58, Cl trace < 0.25, N 8.77.

**Synthesis of (R)-6-Borono-2-(methylamino)-2-(2-(piperidin-1-yl)ethyl)hexanoic Acid (14).** Step 1: **Synthesis of (3R,5R,6S)-5,6-Diphenyl-3-(2-(piperidin-1-yl)ethyl)-3-(4-(4,4,5,5-tetramethyl-1,3,2-dioxaborolan-2-yl)butyl)morpholin-2-one (12).** A solution of (3R,5R,6S)-*tert*-butyl 2-oxo-5,6-diphenyl-3-(2-(piperidin-1-yl)ethyl)-3-(4-(4,4,5,5-tetramethyl-1,3,2-dioxaborolan-2-yl)butyl)morpholine-4-carboxylate, **11** (5.16 g, 7.98 mmol), in DCM (50 mL, 0.16 M) was treated with TFA (10 mL) and stirred at room temperature. After stirring overnight, the solution was concentrated under reduced pressure, dissolved in water, and treated with saturated aqueous NaHCO<sub>3</sub> to pH 9–10. The aqueous solution was extracted with ethyl acetate (3×), dried over anhydrous MgSO<sub>4</sub>, filtered, and concentrated to give (3R,5R,6S)-5,6-diphenyl-3-(2-(piperidin-1-yl)ethyl)-3-(4-(4,4,5,5-tetramethyl-1,3,2-dioxaborolan-2-yl)butyl)morpholin-2-one (**12**) as a colorless oil (3.86 g, 89%) that was used in the next step without further purification.

**Step 2: Synthesis of (3R,5R,6S)-4-Methyl-5,6-diphenyl-3-(2-(piperidin-1-yl)ethyl)-3-(4-(4,4,5,5-tetramethyl-1,3,2-dioxaborolan-2-yl)butyl)morpholin-2-one (13).** A solution of (3R,5R,6S)-5,6-diphenyl-3-(2-(piperidin-1-yl)ethyl)-3-(4-(4,4,5,5-tetramethyl-1,3,2-dioxaborolan-2-yl)butyl)morpholin-2-one, **12** (3.86 g, 7.06 mmol), in THF (50 mL) and acetonitrile (150 mL) was treated with aqueous formaldehyde (5 mL, 37%), acetic acid (1 mL), and NaBH<sub>3</sub>CN (1.01 g) and stirred at room temperature. After stirring overnight, the solution was diluted with saturated aqueous NaHCO<sub>3</sub>, extracted with ethyl acetate (3×), dried over anhydrous MgSO<sub>4</sub>, filtered, and concentrated. Purification by MPLC (0–10% methanol in DCM) gave (3R,5R,6S)-4-methyl-5,6-diphenyl-3-(2-(piperidin-1-yl)ethyl)-3-(4-(4,4,5,5-tetramethyl-1,3,2-dioxaborolan-2-yl)butyl)morpholin-2-one (**13**) as a colorless foam (3.26 g, 82%). <sup>1</sup>H NMR (CDCl<sub>3</sub>, 400 MHz)  $\delta$  7.10–6.98 (m, 6 H), 6.96–6.90 (m, 4 H), 5.92 (d,  $J = 6.8$  Hz, 1 H), 4.06 (d,  $J = 6.8$  Hz, 1 H), 2.58–2.32 (m, 7 H), 2.36 (s, 3 H), 2.06–1.98 (m, 1 H), 1.68–1.36 (m, 12 H), 1.20 (s, 12 H), 0.82 (m, 2 H).

**Step 3: Synthesis of (R)-6-Borono-2-(methylamino)-2-(2-(piperidin-1-yl)ethyl)hexanoic Acid (14).** A solution of (3R,5R,6S)-4-methyl-5,6-diphenyl-3-(2-(piperidin-1-yl)ethyl)-3-(4-(4,4,5,5-tetramethyl-1,3,2-dioxaborolan-2-yl)butyl)morpholin-2-one **13** (3.26 g, 5.82 mmol) in 6 N hydrochloric acid (25 mL) and acetic acid (3 mL) was warmed to 95 °C with stirring overnight. After cooling to

room temperature, the reaction mixture was transferred to a separatory funnel, diluted with deionized water, and washed with DCM. The aqueous layer was concentrated to give the crude boronic acid intermediate as a white foam that was redissolved in 9 N hydrochloric acid and transferred into 20 mL Biotage microwave reactor vials. The vials were capped and then heated, with stirring, in a Biotage Initiator microwave reactor to 170 °C for 40 min. After all vials had been processed, the combined aqueous phase was washed with DCM and concentrated to give (R)-6-borono-2-(methylamino)-2-(2-(piperidin-1-yl)ethyl)hexanoic acid, dihydrochloride monohydrate salt as a very hygroscopic white foam.

Dowex-50WX8-400 ion resin (Aldrich cat# 217514) was washed by stirring successively with MeOH (2×) and water (2×), then briefly suction dried. The crude amino acid was dissolved in water (15 mL) and stirred with the resin at room temperature for 2 h (until LC-MS analysis of the aqueous phase failed to detect the amino acid MH<sup>+</sup> ion). The resin was filtered and then transferred to a sintered chromatography column. Water (~50 mL) was run through the resin column until an aliquot of the collected water fraction failed to give a positive AgNO<sub>3</sub> test (i.e., once all of the chloride had been successfully eluted from the column).

The free-based amino acid was then recovered from the resin by eluting with aqueous 4 N NH<sub>4</sub>OH solution. Fractions were collected until the aqueous solutions were negative for ninhydrin staining and showed no MH<sup>+</sup> ion in LC-MS analysis. The combined product-containing fractions were concentrated to give the purified amino acid as a nonhygroscopic free base hydrate (1.32 g, 76%). <sup>1</sup>H NMR (D<sub>2</sub>O, 400 MHz)  $\delta$  3.57 (t,  $J = 10.4$  Hz, 2 H), 3.40–3.28 (m, 1 H), 3.21–3.12 (m, 1 H), 3.04–2.91 (m, 2 H), 2.71 (s, 3 H), 2.45–2.28 (m, 2 H), 2.05–1.86 (m, 4 H), 1.85–1.66 (m, 3 H), 1.53–1.40 (m, 3 H), 1.39–1.28 (1 H), 1.28–1.15 (m, 1 H), 0.80 (t,  $J = 7.6$  Hz, 2 H); <sup>13</sup>C NMR (D<sub>2</sub>O, 400 MHz)  $\delta$  171.88, 66.75, 53.58, 53.35, 51.52, 31.82, 27.31, 26.61, 24.99, 23.30, 22.88, 22.83, 21.00; ESI-LCMS *m/z* calcd for C<sub>14</sub>H<sub>29</sub>BNO<sub>4</sub>, expected 300.2; found 301.3 (M + H)<sup>+</sup>.

**Synthesis of (R)-2-Amino-6-borono-2-[2-(piperidin-1-yl)ethyl]hexanoic acid (9) via Lithium in Ammonia Reduction. Step 1: Synthesis of (R)-Methyl 2-Allyl-2-(*tert*-butoxycarbonylamino)-6-(4,4,5,5-tetramethyl-1,3,2-dioxaborolan-2-yl)hexanoate (6).** A three-necked RBF equipped with nitrogen inlet tube and dry ice condenser was charged with (3R,5R,6S)-*tert*-butyl 3-allyl-2-oxo-5,6-diphenyl-3-(4-(4,4,5,5-tetramethyl-1,3,2-dioxaborolan-2-yl)butyl)morpholine-4-carboxylate (4.60 g, 8.00 mmol) and THF (10 mL). After cooling the condenser to –78 °C and the flask to –45 °C (CO<sub>2</sub> (s), CH<sub>3</sub>CN), ammonia (80 mL) was condensed into the flask. Once complete, lithium metal (0.55 g, 80 mmol, small pieces) was carefully added over 10 min. After stirring an additional 40 min, the reaction mixture was carefully quenched with NH<sub>4</sub>Cl (s) until the solution became clear. The bath was removed, and the ammonia was allowed to evaporate overnight. The resulting residue was diluted with ethyl acetate and washed successively with 0.5 N HCl and saturated aqueous NaCl, dried over anhydrous MgSO<sub>4</sub>, filtered, and concentrated. Without further purification, the crude product was dissolved in 50% methanol in toluene (80 mL, 0.1 M) and treated with TMS-diazomethane (2.0 M in hexanes) until the pale yellow color persisted. With TLC indicating the reaction complete, the excess TMS-diazomethane was quenched with acetic acid until the solution became clear. The solution was concentrated, diluted with ethyl acetate, washed successively with saturated aqueous NaHCO<sub>3</sub> and saturated aqueous NaCl, dried over anhydrous MgSO<sub>4</sub>, filtered, and concentrated. Purification by MPLC (1–60% ethyl acetate in heptane over 6 CV) gave (R)-methyl 2-allyl-2-(*tert*-butoxycarbonylamino)-6-(4,4,5,5-tetramethyl-1,3,2-dioxaborolan-2-yl)hexanoate as colorless oil (1.9 g, 58%). *R*<sub>f</sub> 0.46 (30% ethyl acetate in heptane); [ $\alpha$ ]<sub>D</sub> +6.51° (c 5.38, CHCl<sub>3</sub>); <sup>1</sup>H NMR (CDCl<sub>3</sub>, 400 MHz)  $\delta$  5.70–5.52 (m, 1 H), 5.49–5.36 (m, 1 H), 5.05 (dd,  $J_1 = 13.8$  Hz,  $J_2 = 1.2$  Hz, 1 H), 3.73 (s, 3 H), 3.09–2.96 (m, 1 H), 2.50 (dd,  $J_1 = 13.8$  Hz,  $J_2 = 7.8$  Hz, 1 H), 2.29–2.10 (m, 1 H), 1.78–1.65 (m, 1 H), 1.43 (s, 9 H), 1.42–1.26 (m, 4 H), 1.23 (s, 12 H), 0.74 (t,  $J = 7.5$  Hz, 2 H); ESI-LCMS *m/z* calcd for C<sub>21</sub>H<sub>38</sub>BNO<sub>6</sub>, expected 411.3; found 412.3 (M + H)<sup>+</sup>.

**Step 2: (R)-Methyl 2-(tert-Butoxycarbonylamino)-2-(2-oxoethyl)-6-(4,4,5,5-tetramethyl-1,3,2-dioxaborolan-2-yl)hexanoate (7).** A solution of (R)-methyl 2-allyl-2-(tert-butoxycarbonylamino)-6-(4,4,5,5-tetramethyl-1,3,2-dioxaborolan-2-yl)hexanoate (1.90 g, 4.62 mmol) in DCM (90 mL, 0.05 M) was cooled to  $-78^{\circ}\text{C}$  and treated with ozone until a pale blue–gray color appeared. After TLC indicated the absence of starting material, the ozone inlet tube was replaced with nitrogen, and nitrogen was bubbled through the solution for 20 min to remove any excess ozone. Triphenylphosphine (3.6 g, 13.8 mmol, 3 equiv) was added in one portion, the cooling bath was removed, and the mixture was stirred for 4 h. The solution was concentrated and purified by MPLC (1–50% ethyl acetate in heptane over 6 CV) and gave (R)-methyl 2-(tert-butoxycarbonylamino)-2-(2-oxoethyl)-6-(4,4,5,5-tetramethyl-1,3,2-dioxaborolan-2-yl)hexanoate as a colorless oil (1.28 g, 67%).  $R_f$  0.55 (30% ethyl acetate in heptane);  $[\alpha]_D^{25} +12.67^{\circ}$  (c 7.50,  $\text{CHCl}_3$ );  $^1\text{H NMR}$  ( $\text{CDCl}_3$ , 300 MHz)  $\delta$  9.66 (s, 1 H), 5.62 (br s, 1 H), 3.75 (s, 3 H), 3.60 (br d,  $J = 17.4$  Hz, 1 H), 2.95 (d,  $J = 17.4$  Hz, 1 H), 2.30–2.15 (m, 1 H), 1.70–1.54 (m, 1 H), 1.40 (s, 9 H), 1.39–1.24 (m, 4 H), 0.74 (t,  $J = 7.8$  Hz, 2 H); ESI-LCMS  $m/z$  calcd for  $\text{C}_{20}\text{H}_{36}\text{BNO}_7$ , expected 413.3; found 414.3 ( $\text{M} + \text{H}$ ) $^+$ ; Anal. Calcd for  $\text{C}_{20}\text{H}_{36}\text{BNO}_7$ , C, 58.12; H, 8.78; N, 3.39. Found C, 58.29; H, 8.94; N, 3.35.

**Step 3: Synthesis of (R)-Methyl 2-((tert-Butoxycarbonyl)amino)-2-(2-(piperidin-1-yl)ethyl)-6-(3,3,4,4-tetramethylborolan-1-yl)hexanoate (8).** A solution of (R)-methyl 2-(tert-butoxycarbonylamino)-2-(2-oxoethyl)-6-(4,4,5,5-tetramethyl-1,3,2-dioxaborolan-2-yl)hexanoate (0.148 g, 0.358 mmol, 1.0 equiv) and piperidine (0.046 g, 0.54 mmol, 1.5 equiv) in 1,2-dichloroethane (0.34 mL, 0.5 M) was treated with sodium triacetoxyborohydride (0.19 g, 0.90 mmol, 2.5 equiv) in one portion. After stirring for 1.5 h, the reaction mixture was quenched with saturated aqueous  $\text{NaHCO}_3$  (1 mL) and stirred for an additional 5 min. The resulting mixture was added to a separatory funnel, diluted with saturated aqueous NaCl (5 mL), and extracted with dichloromethane ( $2 \times 10$  mL). The organic layer was dried over anhydrous  $\text{MgSO}_4$ , filtered, and concentrated under reduced pressure. Purification by flash column chromatography eluting with 5% methanol in chloroform gave (R)-methyl 2-((tert-butoxycarbonyl)amino)-2-(2-(piperidin-1-yl)ethyl)-6-(3,3,4,4-tetramethylborolan-1-yl)hexanoate (8) as a pale yellow oil (0.161 g, 93%).  $R_f$  0.45 (10% methanol in DCM);  $[\alpha]_D^{25} -3.37^{\circ}$  (c 12.05,  $\text{CHCl}_3$ );  $^1\text{H NMR}$  ( $\text{CDCl}_3$ , 300 MHz)  $\delta$  6.10–6.03 (br s, 1 H), 3.63 (s, 3 H), 2.48–2.02 (br s, 6 H), 1.89–1.61 (br s, 4 H), 1.52–1.41 (br s, 4 H), 1.27 (s, 9 H), 1.25–1.22 (br s, 5 H), 1.16 (s, 12 H), 0.98 (br s, 1 H), 0.75 (t,  $J = 7.8$  Hz, 2 H); ESI-LCMS  $m/z$  calcd for  $\text{C}_{25}\text{H}_{47}\text{BN}_2\text{O}_6$ , expected 482.4; found 483.4 ( $\text{M} + \text{H}$ ) $^+$ .

**Step 4: (R)-2-Amino-6-borono-2-(2-(piperidin-1-yl)ethyl)hexanoic Acid (9).** A solution of ester 8 (0.187 g, 0.388 mmol) in 6 N HCl (5 mL) was heated to a gentle reflux for 16 h. After cooling to room temperature, the reaction mixture was transferred to a separatory funnel, diluted with deionized water (5 mL), and washed with DCM ( $3 \times 5$  mL). The aqueous layer was frozen in liquid nitrogen and lyophilized to give amino acid 9 as a dihydrochloride salt (0.124 g, 89%). Analytical data as previously described.

**Pharmacology. Enzyme Preparation.** Recombinant human arginase I cloned in pET-24a (Novagen) was overexpressed and purified using the procedure described previously.<sup>16,17</sup> Briefly, *E. coli* BL21(DE3) strain (Novagen) transformed with the pET-24a plasmid was grown in LB medium at  $37^{\circ}\text{C}$  for 3 h. Protein expression was induced by the addition of 1 mM isopropyl-1-thio- $\beta$ -D-galactopyranoside (IPTG) (Euromedex). The pellet from a 6 L culture was disrupted by sonication in 10 mM Tris-HCl pH 8.0, 10 mM NaCl, 1 mM  $\beta$ -mercaptoethanol, 1 mM  $\text{MnSO}_4$ , and centrifuged at  $4^{\circ}\text{C}$ . Partial purification of arginase I was done by heating at  $60^{\circ}\text{C}$  for 20 min, based on the heat stability of this protein.<sup>18</sup> After heating, the protein was clarified by centrifugation at 45 000 rpm for 30 min. The supernatant was further purified in a hitrap SP FF column of 5 mL (GE Healthcare) equilibrated with 10 mM Tris-HCl pH 8.0, 10 mM NaCl, 1 mM  $\beta$ -mercaptoethanol, 1 mM  $\text{MnSO}_4$ , and eluted with a KCl gradient.

A recombinant, fully active, truncated form of human arginase II was constructed to circumvent aggregation problems observed with the wild-type enzyme.<sup>19,20</sup> The truncation variant  $\Delta\text{M1-V23}/\Delta\text{H331-I354}$  (114 kDa trimer) was created by site-directed mutagenesis using mature human arginase II cDNA. The following primers were used to generate the variant: sense mutagenic primer, TACTAACAT-ATGGTCCACTCCGTTGCTGTGATAGGAGCC, and antisense mutagenic primer, ACTGTACTCGAGTCAATGCCCTCCTTCT-CTTGCTGACCAAAGCTTGAAGC. The truncated variant, cloned in pET23b, was overexpressed as described for arginase I. The pellet from a 6 L culture was disrupted by sonication in a buffer of 10 mM Tris-HCl pH 8.0, 10 mM NaCl, 1 mM  $\beta$ -mercaptoethanol, and 1 mM  $\text{MnSO}_4$ , and centrifuged at  $4^{\circ}\text{C}$ . As for arginase I, partial purification was performed by heating at  $60^{\circ}\text{C}$  for 20 min. After heating, the protein was clarified by centrifugation at 45 000 rpm for 30 min. Then ammonium sulfate was added to the supernatant to 60% saturation, and after centrifugation, the pellet was resuspended in a buffer of 10 mM Tris-HCl pH 8.0, 10 mM NaCl, 1 mM  $\beta$ -mercaptoethanol, and 1 mM  $\text{MnSO}_4$ . The resuspended protein was dialyzed in the same buffer and then applied to an anion exchange, capto Q column of 25 mL (GE Healthcare) and eluted with a KCl gradient.

**Enzymatic Assays.** Arginase converts L-arginine to L-ornithine and urea, and relative arginase activity was determined by measuring urea levels in a colorimetric assay according to published methods.<sup>21</sup> Purified recombinant full length human arginase I protein and recombinant, fully active, truncated form of human arginase II were used to develop 96-well plate human arginase I and arginase II assays. Inhibition of arginase I and arginase II by program compounds was followed spectrophotometrically at 530 nm. The compound to be tested was dissolved in DMSO at an initial concentration that was 50-fold greater than its final concentration in the cuvette. Ten microliters of the stock solution was diluted in 90  $\mu\text{L}$  of the assay buffer that comprised 0.1 M sodium phosphate buffer containing 130 mM NaCl, pH 7.4, to which was added ovalbumin (OVA) at a concentration of 1 mg/mL. Solutions of arginase I and II were prepared in 100 mM sodium phosphate buffer, pH 7.4, containing 1 mg/mL of OVA to give an arginase stock solution at a final concentration of 100 ng/mL.

To each well of a 96-well microtiter plate was added 40  $\mu\text{L}$  of enzyme, 10  $\mu\text{L}$  of the test compound solution, and 10  $\mu\text{L}$  of enzyme substrate solution (L-arginine + manganese sulfate). For wells that were used as positive controls, only the enzyme and its substrate were added, while wells used as negative controls contained only manganese sulfate.

After incubating the microtiter plate at  $37^{\circ}\text{C}$  for 60 min, 150  $\mu\text{L}$  of a urea reagent obtained by combining equal proportions (1:1) of reagents A and B was added to each well of the microtiter plate to stop the reaction. The urea reagent was made just before use by combining Reagent A (10 mM *o*-phthaldialdehyde and 0.4% polyoxyethylene (23) lauryl ether (w/v) in 1.8 M sulfuric acid) with Reagent B (1.3 mM primaquine diphosphate, 0.4% polyoxyethylene (23) lauryl ether (w/v), and 130 mM boric acid in 3.6 M sulfuric acid). After quenching the reaction mixture, the microtiter plate was allowed to stand for an additional 10 min at room temperature in order to allow color development. The inhibition of arginase was computed by measuring the optical density (OD) of the reaction mixture at 530 nm and normalizing the OD value to percent inhibition observed in the control. The normalized OD was then used to generate a concentration–response curve by plotting the normalized OD values against  $\log[\text{concentration}]$  and using regression analysis to compute the  $\text{IC}_{50}$  values.

**Functional Cell Assay. Generation of CHO Cells Stably Expressing Human Arginase I.** The human arginase I (hARGI) expression plasmid was purchased from Origene and subcloned into pcDNA3.1(+) expression vector. Chinese hamster ovary cells (CHO) cells were transfected with hARGI-pcDNA3.1(+) construct using Lipofectamine 2000 according to the manufacturer's instructions (Invitrogen). After 2 days, cells were subjected to selective media containing 800  $\mu\text{g}/\text{mL}$  of Geneticin (Invitrogen). Single colonies of cells expressing hARGI were obtained by using limiting dilutions. Clones were first screened for hARGI expression by Western blotting

and subsequently for arginase activity (see below). The highest expressing clone was chosen to move forward and was maintained in media containing 400  $\mu\text{g}/\text{mL}$  of Geneticin.

**Arginase Activity Measurement in CHO Cells.** Parental CHO and CHO clone stably transfected with hARGI were seeded in a 96-well plate. The next day, the media was replaced with new media containing 5 mM arginine. The cells were incubated at 37 °C. After 24 h, the media was removed and the amount of urea in the media (which serves as an indicator of arginase I activity), was measured using a spectroMAX plate reader at 530 nm as described in the hrARG screening assay. The concentration of urea in each sample was calculated using urea standards with known concentrations of urea.

**Inhibition of Arginase I by Arginase Inhibitors in CHOK Cells Stably Transfected with hARGI.** Parental CHOK and CHOK clones stably transfected with hARGI were seeded in a 96-well plate. The next day, test compounds are added to cells in media containing 5 mM arginine. Each compound was dissolved in PBS and was tested at 0.1, 0.3, 1, 3, 10, 30, 100, and 300  $\mu\text{M}$ . Five wells of a 96-well plate were used for each concentration tested. The cells were incubated at 37 °C for 24 h, after which the amount of urea was measured using a spectroMAX plate reader at 530 nm as described in the hrARG screening assay. The amount of urea generated from parental CHO cells (background) were subtracted from all the values. The urea production in the absence of any compound was considered the maximum urea, and the % inhibition of urea production in the presence of each compound was calculated. The Prism application was used to depict an  $\text{IC}_{50}$  curve and to determine the  $\text{IC}_{50}$  values for each compound.

**Pharmacokinetic Evaluation of Select Inhibitors in Rats.** Single dose pharmacokinetics were evaluated in male Sprague–Dawley rats by intravenous bolus (i.v.) and oral (p.o.) dosing. Three rats were evaluated per dose group. Compound was freshly formulated in 0.9% saline prior to dosing, at 10 mg/mL for i.v. dosing at a dose volume of 1 mL/kg animal body weight, and at 5 mg/mL for p.o. dosing at a dose volume of 2 mL/kg. Animals were fasted overnight prior to dosing, with water given ad libitum. Compound was administered i.v. through a preimplanted cannula or orally by gavage. Food was reintroduced to animals 4 h following dosing. Blood samples were collected through preimplanted cannulae (dual cannulated animals used for i.v. dosing; blood collection separate from dosing cannula) at 0.25 mL per draw, followed by volume replacement with 0.9% saline. Samples were collected at predose 0.083 (i.v. only), 0.25, 0.5, 1, 2, 4, 6, 8, and 24 h following dosing. Blood samples were maintained on ice and centrifuged at 10 000g to obtain plasma. Plasma was frozen at –20 °C prior to analysis. Analysis was performed by LC/MS/MS using Agilent 1100 HPLC pumps with detection on a PESCiex API 4000 Qtrap. Pharmacokinetic evaluation was performed using standard noncompartmental analyses in Phoenix WinNonlin software.

**Efficacy in a Rat Model of Myocardial Ischemia/Reperfusion Injury (MI/RI).** Studies were performed to determine the effect of arginase inhibition on infarct size following MI/RI. Male Sprague–Dawley rats (250–300 g; Charles River Laboratories) were anesthetized with a ketamine/xylazine mixture (100 mg/kg:8 mg/kg, i.p.) and orally intubated with a modified endotracheal tube for mechanical ventilation. The right jugular vein was cannulated using PE-50 tubing and the heart exposed via left thoracotomy in the fourth intercostal space. For animals designated to receive ischemia/reperfusion, a complete occlusion of the left-main coronary artery was achieved by tightening a releasable snare. The pericardium was incised, and a silk 6-0 suture was placed around the vessel and a small portion of the underlying epicardium. Complete coronary occlusion was confirmed visually by noting the prompt and sustained pallor of the anterior wall distal to the ligation site. Occlusion was maintained for 45 min followed by release of the snare; reperfusion was confirmed by prompt return of color to the myocardium distal to the occlusion site. For animals designated as sham, the snare was placed but not tightened. After the surgery, the animals were allowed to recover and returned to their cages, given water and standard rat chow ad libitum and monitored daily until the terminal procedure.

After the completed reperfusion for 2 days, animals were anesthetized with isoflurane (2.5–3%). Following a midline thoracotomy, the heart was arrested in diastole by infusion of cold cardioplegia solution into the left ventricle via a 25 gauge needle inserted into the cardiac apex. The heart with coronary snare suture was excised and mounted onto a modified Langendorff isolated-heart perfusion system. The coronary artery was then reoccluded, and Evans blue/Monastral blue dye was injected into the cannulated aorta for delineation of the area-at-risk. The fresh heart was weighed and the right ventricle removed, and the left ventricle was sectioned into 2 mm thick slices from cardiac apex to base and incubated with triphenyltetrazolium chloride (1% in PBS) at 37 °C for 15–30 min followed by immersion in 10% formalin in phosphate buffered saline. Fixed slices were digitally scanned for image analysis using Image J software.

The study tested the effect of compound **9** (100 mg/kg, i.v.) and compound **15** (100 mg/kg, i.v.), the inactive enantiomer of compound **9**. For both studies, compounds were administered as a bolus 15 min before occlusion of the coronary artery. Results are expressed as mean  $\pm$  SEM; statistical analysis was conducted using X with  $p < 0.05$  regarded as significant. The MI/RI study was conducted in the laboratory of Dr. Francisco Villarreal at the University of California, San Diego, on a fee-for-service basis.

**X-ray Crystallography. Crystallization of Human Arginase I and the Truncation Variant  $\Delta\text{M1-V23}/\Delta\text{H331-I354}$  of Human Arginase II.** Crystals of the native enzyme arginase I were obtained by vapor diffusion method at 4 °C. Drops containing 4.0  $\mu\text{L}$  of enzyme solution [5 mg/mL human arginase I, 10 mM Tris-HCl pH 7.5, 10 mM NaCl, 1 mM  $\beta$ -mercaptoethanol, and 0.2 mM  $\text{MnSO}_4$ ] and 4  $\mu\text{L}$  of precipitant solution [100 mM malonic acid, imidazol, boric system pH5, and 25% polyethylene glycol (PEG) 1500] were equilibrated against a 1 mL reservoir of precipitant solution. Rod-like crystals appeared in approximately one week and grew to typical dimensions of 0.1 mm  $\times$  0.1 mm  $\times$  0.4 mm. Soaking was used to obtain crystals of the arginase I–inhibitor complexes.<sup>22–24</sup> Native crystals of arginase I were transferred in a drop containing 15 mM compounds **9** or **14** dissolved in the precipitant solution (100 mM malonic acid, imidazol, boric system pH 5, and 25% PEG 1500). The crystals were soaked during one week then cryoprotected by the precipitant solution containing 30% ethylene glycol prior to flash cooling in liquid nitrogen. Crystals of the human arginase II–inhibitor complexes were obtained by cocrystallization of arginase II with 2 mM compound **9** or **14**. Crystals were obtained by vapor diffusion method at 4 °C. Protein was concentrated at 5 mg/mL in 10 mM Tris-HCl pH 8.0, 10 mM NaCl, 1 mM  $\beta$ -mercaptoethanol, and 0.2 mM  $\text{MnSO}_4$ . Crystals were obtained under the H3 condition of a Silver Bullets screen (Hampton Research) using Tacsimate in the reservoir. Crystals appeared in a few days and grew to typical dimensions of 0.3 mm  $\times$  0.3 mm  $\times$  0.5 mm. They were cryoprotected by the reservoir solution containing 30% ethylene glycol prior to flash cooling in liquid nitrogen.

**Data Collection.** For both crystals of human arginase I– and II–compound **9** complexes, X-ray diffraction data were collected, respectively, at 1.30 and 1.60 Å resolution on X06DA beamline at the synchrotron Swiss Light Source (SLS), Switzerland. The crystals belong to space group  $P3$  with unit cell parameters of  $a = b = 90.14$  Å and  $c = 69.33$  Å and to space group  $P4_22_2$  with unit cell parameters of  $a = b = 127.74$  Å and  $c = 159.11$  Å.

For both crystals of the arginase I– and II–compound **14** complexes, X-ray diffraction data were collected, respectively, at 1.45 and 1.80 Å resolution on X06SA beamline at the synchrotron SLS. The crystals belong to space group  $P3$  with unit cell parameters of  $a = b = 90.32$  Å and  $c = 69.53$  Å and to space group  $P4_22_2$  with unit cell parameters of  $a = b = 127.81$  Å and  $c = 159.09$  Å. All data were processed with HKL2000.<sup>25</sup>

Both data collection and refinement statistics for the four complexes are included as Supporting Information.

**Structural Refinement.** The structures of all complexes arginases I and II with inhibitors **9** and **14** were solved by molecular replacement with AMORE using the structure of a rat arginase protein complexed

with a boronic inhibitor (Protein Data Bank ID: 1D3V) as a search model, against 8–3 Å data. Clear solutions were always obtained.

Further crystallographic refinement involved several repeated cycles of conjugate gradient energy minimization and temperature factor refinement, performed with the CCP4 suite.<sup>26</sup> Amino acid side-chains were fitted into 2Fo–Fc and Fo–Fc electron density maps. The final Fo–Fc maps indicated a clear electron density for each different inhibitor. Water molecules were fitted into difference maps, and riding H-atoms were introduced in the final cycles. The programs Phenix<sup>27</sup> and Coot were used for refinement and fitting the models to the electron density.<sup>28</sup> Both arginase I complexes were solved from twin crystals and were refined according to the twin law “-h, -k, l”. Refinement statistics are presented in Table 1. The atomic coordinates have been deposited in the Protein Data Bank (PDB IDs: 4HWW, 4HXQ, 4HZE and 4I06) and will be released upon publication. The inhibitor binding sites were analyzed using Coot,<sup>28</sup> while figures were generated with the PyMOL Molecular Graphics System (Delano Scientific LLC).

## ■ ASSOCIATED CONTENT

### ■ Supporting Information

<sup>1</sup>H NMR and <sup>13</sup>C NMR spectra, LC MS/MS data, analytical HPLC chromatograms, chiral HPLC chromatograms, and X-ray crystallography data collection and refinement statistics. This material is available free of charge via the Internet at <http://pubs.acs.org>.

## ■ AUTHOR INFORMATION

### Corresponding Author

\*Phone: 203-494-1672. E-mail: [mvzandt@snet.net](mailto:mvzandt@snet.net).

### Notes

The authors declare no competing financial interest.

## ■ ACKNOWLEDGMENTS

We thank Mars, Incorporated, for their helpful discussions and generous financial support of this program. We also thank the IGBMC Structural genomics platform staff, in particular Pierre Poussin-Courmontagne and Alastair McEwen. We thank Drs. Di Constanzo, Centeno, and Velazquez for the clone of arginase I and Drs. Cederbaum, Deignan, and Gotoh for the clone of arginase II. The crystallographic experiments were performed on the X06SA and X06DA beamlines at the Swiss Light Source, Paul Scherrer Institut, Villigen, Switzerland. In particular, we thank Takashi Tomizaki, Vincent Olieric, Anuschka Pauluhn, Christian Stirnimann, and Meitian Wang for their help in the beamline. E.I.H. is member of the Carrera del Investigador, Conicet, Argentina. This work was supported by the Centre National de la Recherche Scientifique (CNRS), the Institut National de la Santé et de la Recherche Médicale, the Hôpital Universitaire de Strasbourg (H.U.S.), and the Université de Strasbourg. Finally, we thank Dr. Francisco Villarreal at the University of California, San Diego, for his efforts in conducting the MI/RI experiments.

## ■ ABBREVIATIONS USED

AAR, area at risk; ABH, 2-(S)-amino-6-boronohexanoic acid; Arg, arginase; CHO, Chinese hamster ovary; DCM, dichloromethane; DMA, dimethylacetamide; DME, 1,2-dimethoxyethane; DMF, dimethylformamide; DMSO, dimethylsulfoxide; ELSD, evaporative light scattering detector; HMPA, hexamethylphosphoramide; IPC, intermittent preconditioning; KHMDs, potassium hexamethyldisilazane; LiHMDs, lithium hexamethyldisilazane; MeOH, methanol; MI/RI, myocardial ischemia/reperfusion injury; NaHMDs, sodium hexamethyldi-

silazane; NO, nitric oxide; NOS, nitric oxide synthase; SAR, structure–activity relationship; TFA, trifluoroacetic acid; THF, tetrahydrofuran; TMEDA, tetramethylethylenediamine; TMSCH<sub>2</sub>N<sub>2</sub>, trimethylsilyl-diazomethane

## ■ REFERENCES

- (1) Zweier, J. L.; Talukder, M. A. H. The role of oxidants and free radicals in reperfusion injury. *Cardiovasc. Res.* **2006**, *70*, 181–190.
- (2) Alkaitis, M. S.; Crabtree, M. J. Recoupling the cardiac nitric oxide synthases: tetrahydrobiopterin synthesis and recycling. *Curr. Heart Failure Rep.* **2012**, *9*, 200–210.
- (3) Vinten-Johansen, J. Involvement of neutrophils in the pathogenesis of lethal myocardial reperfusion injury. *Cardiovasc. Res.* **2004**, *61*, 481–497.
- (4) Eeffing, F.; Rensing, B.; Wigman, J.; Pannekoek, W. J.; Liu, W. M.; Cramer, M. J.; Lips, D. J.; Doevandans. Role of apoptosis in reperfusion injury. *Cardiovasc. Res.* **2004**, *61*, 414–426.
- (5) Liao, Y.-H.; Xia, N.; Zhou, S.-F.; Tang, T.-T.; Yan, X.-X.; Lv, B.-J.; Nie, S.-F.; Wang, J.; Iwakura, Y.; Xiao, H.; Yuan, J.; Jevallie, H.; Wei, F.; Shi, G.-P.; Cheng, X. Interleukin-17A contributes to myocardial ischemia/reperfusion injury by regulating cardiomyocyte apoptosis and neutrophil infiltration. *J. Am. Coll. Cardiol.* **2012**, *59*, 420–429.
- (6) Ruiz-Meana, M.; Garcia-Dorado, D.; Hofstaetter, B.; Piper, H. M.; Soler-Soler, J. Propagation of cardiomyocyte hypercontracture by passage of Na<sup>+</sup> through gap junctions. *Circ. Res.* **1999**, *85*, 280–287.
- (7) Hoffman, J. W.; Gilbert, T. B.; Poston, R. S.; Silldorff, E. P. Myocardial reperfusion injury: etiology, mechanisms, and therapies. *J. Extra-Corpor. Technol.* **2004**, *36*, 391–411.
- (8) Gonon, A. T.; Jung, C.; Katz, A.; Westerblad, H.; Shemyakin, A.; Sjoquist, O.; Lundberg, J. O.; Pernow, J. Local arginase inhibition during early reperfusion mediates cardioprotection via increased nitric oxide production. *PLoS One* **2012**, *7*, e42038.
- (9) Rastaldo, R.; Pagliaro, P.; Cappello, P.; Penna, C.; Mancardi, D.; Westerhof, N.; Losano, G. Nitric oxide and cardiac function. *Life Sci.* **2007**, *81*, 779–793.
- (10) Shantz, L. M.; Giordano, E. Polyamine Metabolism and the Hypertrophic Heart. In *Polyamine Cell Signaling: Physiology, Pharmacology, and Cancer Research*; Wang, J.-Y.; Casero, R. A., Jr., Eds; Humana Press: Totowa, NJ, 2006; pp 123–137.
- (11) Ash, D. E.; Scolnick, L. R.; Kanyo, Z. F.; Vockley, J. G.; Cederbaum, S. D.; Christianson, D. W. Molecular basis of hyperargininemia: structure-function consequences of mutations in human liver arginase. *Mol. Genet. Metab.* **1998**, *64*, 243–249.
- (12) Santhanam, L.; Christianson, D. W.; Nyhan, D.; Berkowitz, D. E. Arginase and vascular aging. *J. Appl. Physiol.* **2008**, *105*, 1632–1642.
- (13) Ryoo, S.; Gupta, G.; Benjo, A.; Lim, H. K.; Camara, A.; Sikka, G.; Sohi, J.; Santhanam, L.; Soucy, K.; Tuday, E.; Baraban, E.; Lies, M.; Gerstenblith, G.; Nyhan, D.; Shoukas, A.; Christianson, D. W.; Alp, N. J.; Champion, H. C.; Huso, D. Berkowitz. endothelial arginase II: a novel target for treatment of atherosclerosis. *Circ. Res.* **2008**, *102*, 923–932.
- (14) Golebiowski, A.; Beckett, R. P.; Van Zandt, M.; Ji, M. K.; Whitehouse, D.; Ryder, T.; Jagdmann, E.; Andreoli, M.; Mazur, A.; Padmanilayam, M.; Cousido-Siah, A.; Mitschler, A.; Ruiz, F. X.; Podjarny, A.; Schroeter, H. 2-Substituted-2-amino-6-boronohexanoic acids as arginase inhibitors. *Biorg. Med. Chem. Lett.* **2013**, in press.
- (15) Dastlik, K. A.; Sundermeier, U.; Johns, D. M.; Chen, Y.; Williams, R. M. An improved synthesis of optically pure 4-Boc-5,6-diphenylmorpholin-2-one and 4-Cbz-5,6-diphenylmorpholin-2-one. *Synlett* **2005**, 693–696.
- (16) Mora, A.; Rangel, M. D. A.; Fuentes, J. M.; Soler, G.; Centeno, F. Implications of the S-shaped domain in the quaternary structure of human arginase. *Biochim. Biophys. Acta* **2000**, *1476*, 181–190.
- (17) Di Costanzo, L.; Sabio, G.; Mora, A.; Rodriguez, P. C.; Ochoa, A. C.; Centeno, F.; Christianson, D. W. Crystal structure of human arginase I at 1.29 Å resolution and exploration of inhibition in the immune response. *Proc. Natl. Acad. Sci. U.S.A.* **2005**, *102*, 13058–13063.

(18) Scolnick, L. R.; Kanyo, Z. F.; Cavalli, R. C.; Ash, D. E.; Christianson, D. W. Altering the binuclear manganese cluster of arginase diminishes thermostability and catalytic function. *Biochemistry* **1997**, *36*, 10558–10565.

(19) Colleluori, D. M.; Morris, S. M.; Ash, D. E. Expression, purification, and characterization of human type II arginase. *Arch. Biochem. Biophys.* **2001**, *389*, 135–143.

(20) Cama, E.; Colleluori, D. M.; Emig, F. A.; Shin, H.; Kim, S. W.; Kim, N. N.; Traish, A. M.; Ash, D. E.; Christianson, D. W. Human arginase II: crystal structure and physiological role in male and female sexual arousal. *Biochemistry* **2003**, *42*, 8445–8451.

(21) Jung, D.; Biggs, H.; Erikson, J.; Ledyard, P. U. *Clin. Chem.* **1975**, *21*, 1136.

(22) Cama, E.; Pethe, S.; Boucher, J. L.; Han, S.; Emig, F. A.; Ash, D. E.; Viola, R. E.; Mansuy, D.; Christianson, D. W. Inhibitor coordination interactions in the binuclear manganese cluster of arginase. *Biochemistry* **2004**, *43*, 8987–8999.

(23) Cox, J. D.; Cama, E.; Colleluori, D. M.; Pethe, S.; Boucher, J. L.; Mansuy, D.; Ash, D. E.; Christianson, D. W. Mechanistic and metabolic inferences from the binding of substrate analogues and products to arginase. *Biochemistry* **2001**, *40*, 2689–2701.

(24) Shishova, E. Y.; Di Costanzo, L.; Emig, F. A.; Ash, D. E.; Christianson, D. W. Probing the specificity determinants of amino acid recognition by arginase. *Biochemistry* **2009**, *48*, 121–131.

(25) Otwinowski, Z.; Minor, W. Processing of X-ray Diffraction Data Collected in Oscillation Mode. *Methods in Enzymology, Volume 276: Macromolecular Crystallography, Part A*, Carter, C. W., Jr., Sweet, R. M., Eds.; Academic Press: New York, 1997; Vol. 276, pp 307–326.

(26) Winn, M. D.; Ballard, C. C.; Cowtan, K. D.; Dodson, E. J.; Emsley, P.; Evans, P. R.; Keegan, R. M.; Krissinel, E. B.; Leslie, A. G.; McCoy, A.; McNicholas, S. J.; Murshudov, G. N.; Pannu, N. S.; Potterton, E. A.; Powell, H. R.; Read, R. J.; Vagin, A.; Wilson, K. S. *Acta Crystallogr., Sect. D: Biol. Crystallogr.* **2011**, *67*, 235–242.

(27) Adams, P. D.; Afonine, P. V.; Bunkoczi, G.; Chen, V. B.; Davis, I. W.; Echols, N.; Headd, J. J.; Hung, L. W.; Kapral, G. J.; Grosse-Kunstleve, R. W.; McCoy, A. J.; Moriarty, N. W.; Oeffner, R.; Read, R. J.; Richardson, D. C.; Richardson, J. S.; Terwilliger, T. C.; Zwart, P. H. *Acta Crystallogr., Sect. D: Biol. Crystallogr.* **2010**, *66*, 213–221.

(28) Emsley, P.; Lohkamp, B.; Scott, W.; Cowtan, K. Features and Development of Coot. *Acta Crystallogr., Sect. D: Biol. Crystallogr.* **2010**, *66*, 486–501.